Spring 2017

Investigation of AI-2 Binding to the Quorum Sensing Receptor LsrB

Meghann R. Kasal , '17

Investigation of AI-2 Binding to the Quorum Sensing Receptor LsrB

Meghann Kasal
Senior Course Research Thesis, April 2017
Department of Chemistry and Biochemistry
Swarthmore College, Swarthmore, PA
Advisor: Stephen T. Miller

Table of Contents

Acknowledgements

I would first like to thank my research advisor, Stephen Miller, for the opportunity to conduct meaningful and challenging biochemistry research and for guiding me to become a better scientist over my two years in the lab. I would also like to thank my lab mates past and present, Emily Gale, Audrey Allen, Jason Hua, Elijah Kissman, Nicholas Petty, and Judy Al, for their support and entertainment in the lab. I would like to specially thank Inês Torcato, with whom I have collaborated for almost a year and who constantly gives me scientific, and other, advice. I want to thank my family, who has given me all the opportunities I need to become a successful scientist, and my friends, who have supported me through all my lab endeavors. Furthermore, I would like to give thanks to Silvia Porello and Liliya Yatsunyk for their feedback and participation on my thesis committee. Finally, I would like to thank Swarthmore College for awarding me the Mayer Davidson '57 Summer Research Fellowship and the Frances Velay Womens Science Research Fellowship, which allowed me to conduct research over two summers.

Abstract

Bacterial cell-cell communication, known as quorum sensing, is a density-dependent phenomenon that regulates multicellular behaviors such as bioluminescence and virulence. Interspecies quorum sensing is mediated by a signal known as autoinducer-2 (AI-2), which belongs to a family of molecules derived from 4,5-Dihydroxy-2,3-pentanedione (DPD), a key metabolic product of the enzyme LuxS. AI-2 is recognized by many bacteria that belong to several phyla, including *Enterobacteriaceae*, *Rhizobiaceae*, and *Bacillaceae*, as a non-borated cyclic derivative of DPD known as (2*R*,4*S*)-2-methyl-2,3,3,4-tetrahydroxytetrahydrofuran (*R*-THMF). Building on previous research, we have recently identified several novel LsrB orthologs through sequence alignments and fold-prediction software. We showed that *Thermobacillus composti* and *Clostridium saccharobutylicium* have functional AI-2 receptors despite variations in the binding site residues as compared to known LsrB proteins. Furthermore, we obtained an X-ray crystal structure of *C. saccharobutylicium* LsrB which indicated that the binding site superimposes well onto a known receptor from *Salmonella typhimurium*. We optimized a purification protocol for each receptor and have begun to conduct ITC experiments to assay the differences in binding affinity across species and to determine which residues are critical for AI-2 recognition. Finally, crystallization trials have identified potential conditions to yield crystals *T. composti* LsrB, which will be explored in the future to elucidate the protein-ligand binding interactions.

Chapter 1. Introduction

The phenomenon of bacterial cell-cell signaling and communication, known as quorum sensing, was first discovered and described in the bioluminescent marine bacterium *Vibrio fischeri*.[1,2] These bacteria flourish in symbiotic relationships with eukaryotic hosts, such as the sepiolid squid *Euprymna scolopes*, that have evolved to benefit from bioluminescence for survival.[3] Light emission by the *V. fischeri* bacteria is regulated by an autoinducer signal which initiates transcription of the enzymes required for bioluminescence.

In high cell density cultures, like those found in the light organs of *E. scolopes* when the squid is camouflaging itself, *V. fischeri* respond to an accumulation of secreted autoinducer signal molecules by expressing the luciferase operon (*luxCDABE*).[4] The luciferase enzyme, composed of subunits LuxA and LuxB, catalyzes the oxidation of reduced flavin mononucleotide with molecular oxygen, leading to bioluminescence.[5] The synthase, LuxI, produces the autoinducer signal that is recognized by the constitutively expressed quorum sensing receptor, LuxR.[4] Binding of the autoinducer signal to LuxR promotes the expression of the *lux* genes in a positive feedback loop.[6] For the bacteria to simultaneously alter gene expression and produce light, the secreted signal molecule must reach a threshold concentration in the high cell density culture.[2] Thus, *V. fischeri* communicate through production and uptake of a small autoinducer signal molecule which results in coordinated gene expression and community-wide behavioral regulation.

Intraspecies quorum sensing that is similar to the canonical example in *V. fischeri* has since been identified in many other Gram-negative bacteria in the regulation of diverse community-wide behaviors including expression of virulence factors,[7] formation of biofilms,[8] and production of

antibiotics.[9] These quorum sensing processes are mediated by acylated homoserine lactone (HSL) signal molecules that are produced and bound by the regulatory proteins LuxI and LuxR, respectively.[10] Each species binds a specific and unique HSL autoinducer that forms a complex with LuxR-type proteins in the cytoplasm, activating target gene transcription.[11]

Other cases of intraspecies quorum sensing have also been described for Gram-positive bacteria, which communicate through a peptide autoinducer. The signal peptides are secreted through ATP-binding cassette (ABC) transporters and accumulate extracellularly at high cell density leading to detection by sensory kinases that initiate a two-component phosphorylation/dephosphorylation signaling circuit that regulates community behaviors.[10,12] Through intraspecies quorum sensing, fluctuations in cell population density are coupled to the regulation of gene expression and coordinated behavioral changes that are beneficial to the bacteria.

The related marine bacterium *Vibrio harveyi* uses several quorum sensing circuits to regulate bioluminescence.[13] *V. harveyi* predominantly respond to HSL signal molecules to express the luciferase operon and produce light,[13] but they also recognize to a separate secreted autoinducer that regulates the production of light through a distinct quorum sensing circuit.[2] The autoinducer signal that mediates non-canonical *V. harveyi* cell-cell communication is a furanosyl borate diester molecule known as autoinducer-2 (AI-2).[14] The AI-2 synthase, LuxS,[15] has been identified in dozens of Gram-negative and Gram-positive bacteria,[16] which suggests that many bacterial species generate AI-2 activity. The periplasmic binding protein for AI-2, LuxP,[17] has also been found in many other *Vibrio* species.[10] Moreover, *V. harveyi* respond to the autoinducer signal produced by other bacteria, facilitating interspecies cell-cell communication.[18] By sensing the environment for

HSL and AI-2 signals, *V. harveyi* maintain intraspecies and interspecies communication circuits that lead to regulation of bioluminescence.

The AI-2 signal molecule utilized by *V. harveyi* and other marine bacteria for interspecies communication exists in a borated form, (2*S*,4*S*)-2-methyl-2,3,3,4-tetrahydroxytetrahydrofuran-borate (*S*-THMF-borate),[14] which is derived from 4,5-Dihydroxy-2,3-pentanedione (DPD), a key metabolic product of the enzyme LuxS (Figure 1.1).[19] In marine environments where boric acid is present in high concentrations,[20] DPD predominantly cyclizes to *S*-THMF and complexes with borate to form the signal molecule recognized by *V. harveyi*.[13] However, many terrestrial bacteria that live in boron-depleted environments[21] like *Salmonella* and *Escherichia* species also respond to AI-2,[13] suggesting that DPD exists in an equilibrium between *S*-THMF-borate and another active form of DPD (Figure 1.1).

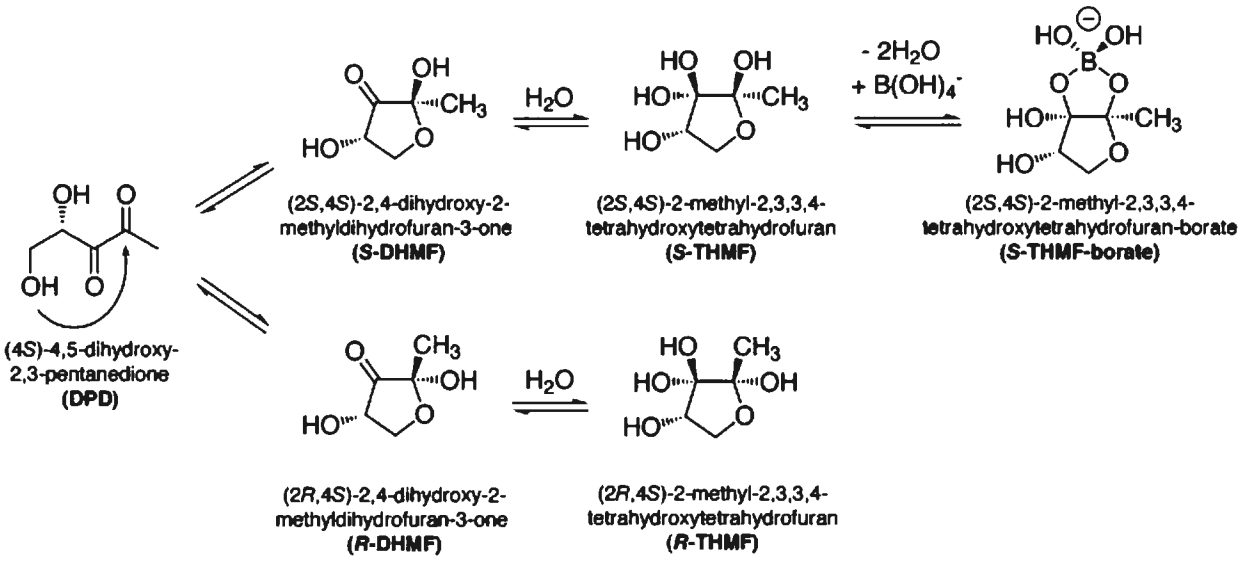

Figure 1.1 *Equilibrium between distinct forms of AI-2 recognized by LuxP (S-THMF-borate) and LsrB (R-THMF). Adapted from reference 19.*

Since the determination that *V. harveyi* binds *S*-THMF-borate, research has been conducted to determine the active form of AI-2 recognized by bacteria that live in boron-depleted environments. A crystal structure of the AI-2 receptor from *Salmonella typhimurium* revealed that a chemically distinct form of the signal molecule binds to a novel quorum sensing receptor known as LsrB.[19] The LuxS-regulated (Lsr) receptor protein in *S. typhimurium* recognizes a non-borated, cyclic derivative of DPD, (2*R*,4*S*)-2-methyl-2,3,3,4-tetrahydroxytetrahydrofuran (*R*-THMF) (Figure 1.1).[19] The concentration of boric acid mediates the equilibrium between *R*-THMF and *S*-THMF-borate, the two known active forms of AI-2 that bind the AI-2 receptors LsrB and LuxP, respectively.[19] Thus, the AI-2 signal molecule is regarded as a "universal" signal because it is composed of a family of interconverting molecules that are produced and recognized by various bacterial species in interspecies quorum sensing.[22]

The mechanism of signal production, uptake, and processing of *R*-THMF has been elucidated in *S. typhimurium*, bacteria that are thought to use AI-2-mediated quorum sensing to interfere with the signaling of other bacterial species.[22] Upon binding to LsrB, the signal molecule is internalized through a transmembrane ATP binding cassette (ABC) transporter complex composed of LsrA, LsrC, and LsrD (Figure 1.2).[23] AI-2 is then phosphorylated by LsrK, which prevents the signal from leaving the cell and depletes AI-2 from the extracellular environment.[22] Furthermore, the phosphorylated form of AI-2 (P-AI-2) binds to the transcriptional repressor, LsrR, inducing expression of the *lsr* operon, which encodes for the genes *lsrACDBFGE*. Derepression of the operon is essential for the downstream processing of P-AI-2 and subsequent quenching of the quorum sensing response. LsrG catalyzes the isomerization of P-DPD to 3,4,4-trihydroxy-2-pentanone-5-phosphate (P-TPO), a reaction that is necessary for the sensitivity of the Lsr system

in AI-2-mediated quorum sensing.[24] Mutants with an *lsrG* deletion accumulate as much as ten times more P-DPD than wild-type bacteria, leading to high levels of expression of the *lsr* operon. The terminal enzyme in the downstream processing of P-AI-2, LsrF, transfers an acetyl group from P-TPO to Coenzyme A (CoASH), yielding dihydroxyacetone phosphate (DHAP) and acetyl-Coenzyme A (acetyl-CoA).[25] The final products of AI-2 signal processing, DHAP and acetyl-CoA, are metabolically significant substrates, suggesting a physiological function for the quenching of AI-2 mediated quorum sensing.[23,26]

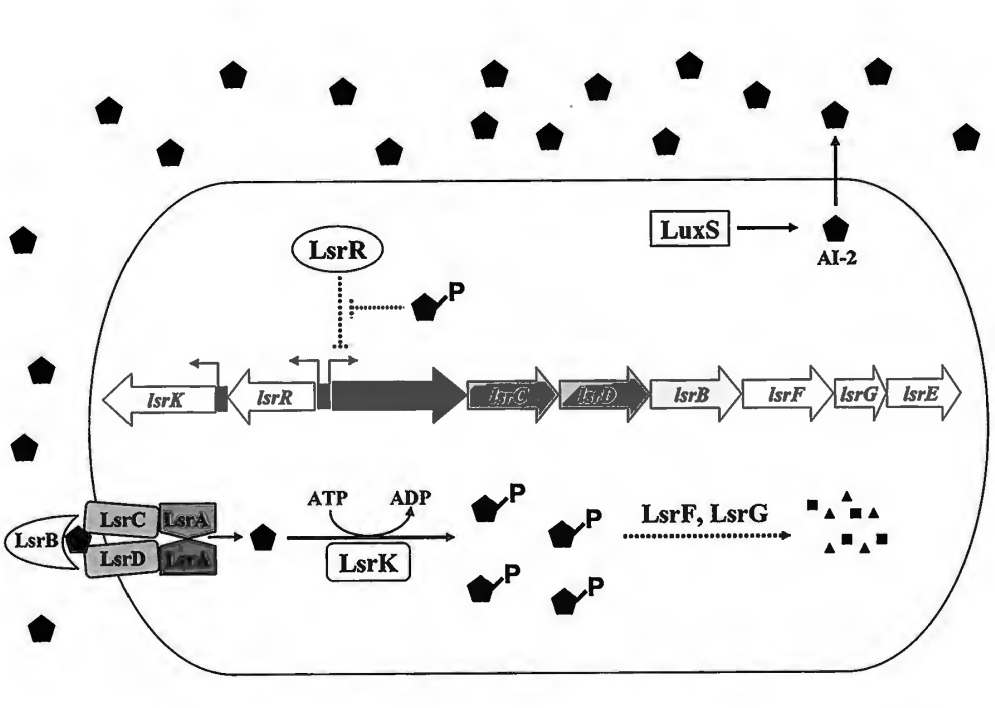

Figure 1.2 *Model of AI-2 production, internalization, and processing. (⬟) AI-2. Adapted from reference 23.*

Previous research has been conducted to expand the repertoire of known LsrB receptors and, as such, identify previously-unknown bacteria that engage in interspecies quorum sensing.[27] Two groups of LsrB orthologs have been established: functional LsrB-like receptors and orthologs that

have some other function.[27] The LsrB-like receptors have high sequence identity with *S. typhimurium* LsrB and complete conservation of the binding site residues. These functional receptors belong to a diverse group of bacteria across several phyla including *Enterobacteriaceae*, *Rhizobiaceae*, and *Bacillaceae*. The orthologs that do not display quorum sensing functionality have low sequence identity, between 27–36%, with *S. typhimurium* LsrB and several mutations of the predicted binding site residues.[27] Consequently, these orthologs are unable to function as LsrB-type receptors and do not bind AI-2. Furthermore, these bacteria lack other essential genes in the *lsr* operon that encode for AI-2 internalization and processing.

More recently, a previously uncharacterized third group of LsrB orthologs has been identified. These orthologs have intermediate sequence identity to *Bacillus cereus* LsrB, a known AI-2 receptor, and partial conservation of binding site residues. We have begun exploring this previously-uncharacterized group of orthologs to determine if they are functional LsrB-type receptors that are involved in interspecies quorum sensing.

Chapter 2. Identification of Novel LsrB AI-2 receptors

Structural comparison of AI-2 bound to the receptors of *Salmonella typhimurium* LsrB and *Vibrio harveyi* LuxP revealed that two chemically distinct forms of the signal molecule bind to each sensory protein.[19] The active form of AI-2 that interacts with LsrB, *R*-THMF, is a non-borated diastereomer of the LuxP signal, *S*-THMF-borate (Figure 1.1). The formation of the *R*-THMF or *S*-THMF isomers is mediated by an equilibrium through DPD, which is synthesized by LuxS,[15,19] therefore these ligands are said to belong to the AI-2 family of signal molecules. Moreover, structural differences between the LsrB and LuxP receptors determine the form of AI-2 that is recognized,[19] which can affect the responsiveness of the bacteria to the signal molecule depending on the chemical environment. The characterization of a novel, biologically active form of AI-2 led to an initial search for additional LsrB-type receptors that bind *R*-THMF. LsrB orthologs have since been described in a diverse set of bacterial species from phylogenetically distinct families, including *Enterobacteriaceae*, *Rhizobiaceae*, and *Bacillaceae*, adding to the repertoire of known AI-2-responsive bacteria and AI-2 receptors.[27]

To find these LsrB orthologs initially, all available complete genomes (KEGG) were queried with the amino acid sequence of *S. typhimurium* LsrB. The search identified several protein hits from a variety of bacterial species with high sequence identity to the known LsrB receptor and complete conservation of the binding site residues, as determined by sequence alignments and structural prediction models.[27] These bacteria also have orthologs of the complete *lsr* operon, which suggests that they can actively respond to AI-2 in their environment through recognition, internalization, and processing of the signal molecule.[27] Additionally, the query identified a second group of bacteria that lacks several gene sequences from the *lsr* operon and whose LsrB orthologs have low

sequence identity (less than 36%) and several mutations in the binding site as compared to *S. typhimurium* LsrB.[27] These LsrB orthologs were determined to have a function other than AI-2 recognition and uptake, because they were unable to bind and internalize the signal molecule.[27]

Since the previous characterization of the two groups of LsrB orthologs, the all available complete genomes (KEGG) have been queried again, but using the amino acid sequence of *Bacillus cereus* LsrB, a functional receptor identified in the initial investigations into LsrB orthologs[27] that belongs to the Firmicutes. From this search, a third group of LsrB orthologs has been identified that have an intermediate sequence identity, between 36–56%, to *B. cereus* LsrB and only partial conservation of binding site residues. We narrowed the hundreds of search results to only bacteria in the Firmicute phylum because of previous work showing that, after antibiotic-induced dysbiosis, the abundance of Firmicutes in the murine gut increases when AI-2-producing *E. coli* are present.[28] As a result, the ratio of Firmicutes to Bacteroidetes, another phylum of bacteria commonly found in the gut, is greater which helps to restore microbiota function. Manipulation of the AI-2 quorum sensing signal in the gut, thus, has the potential to modify microbiota composition, which has a major influence on host health. Additionally, the manipulation of the AI-2 signal could be used in conjunction with or instead of antibiotics to promote the growth of beneficial bacteria in the gut and to suppress the proliferation of bacteria that are dangerous for human health.

We proposed that several of these orthologs from Firmicute bacteria are functional LsrB-like receptors despite predicted variations in the binding site. Moreover, approximately 83% of the currently sequenced Firmicute genomes possess a homolog of the LuxS synthase, suggesting that they communicate through AI-2 signaling.[28] Consequently, we have begun to determine if these

orthologs bind and internalize AI-2 by investigating the binding of the LsrB orthologs from *Clostridium saccharobutylicium* and *Thermobacillus composti*, two bacterial species belonging to the Firmicute phylum identified in this secondary search.

MATERIALS AND METHODS

KEGG Sequence Alignments

The amino acid sequence of *Bacillus cereus* LsrB was aligned against all completely sequenced genomes deposited in the Kyoto Encyclopedia of Genes and Genomes (KEGG)[29] using the bidirectional best-best hits algorithm.* The amino acid, rather than nucleotide, sequence was used in the search because it is less prone to errors from silent mutations. We identified many possible receptors, but focused on Firmicute bacteria based off previous work showing that the colonization of Firmicutes increases in the presence of AI-2 in the murine gut after dysbiosis.[28] Thus, the experimental focus was narrowed to bacterial LsrB homologues from *Thermobacillus composti* and *Clostridium saccharobutylicium*, which belong to the Firmicute phylum.

Structural Predictions and Alignments

Predicted structures for LsrB from *T. composti* and *C. saccharobutylicium* were generated from primary sequences using the Protein Homology/analogY Recognition Engine V 2.0 Server (PHYRE^2)[31] and visualized using the Crystallographic Object-Oriented Toolkit (Coot). Structural alignments were performed with the predicted LsrB structures against a published structure of LsrB from *Salmonella typhimurium* crystallized with AI-2 bound (PDB: 1TJY). The binding site

*The algorithm compares gene *x* from genome *A* to gene *y* from genome *B*. The bidirectional best hits are determined when *x* is compared to B, finding *y* as top-scoring, and *y* is compared to A, finding *x* as top-scoring.[30]

residues of *S. typhimurium* LsrB were determined to be Lys35, Asp116, Asp166, Gln167, Pro220, and Ala222. These residues were used to assess the level of conservation in the active site of the putative LsrB receptors.[19] PyMOL Molecular Graphics System (PyMOL) was used to visualize models of the orthologs (Figures 2.1 and 2.3).

Determination of N-terminal deletions of LsrB Constructs

N-terminal deletion of the signal peptide in the recombinant protein was required to solubilize the protein as well as mimic the naturally derived protein product during recombinant protein expression.[32] Initially, signal peptide prediction software (SignalP) was used to identify the cleavage site for *T. composti* and *C. saccharobutylicium* LsrB (Supplemental Figure 1).[33] For *C. saccharobutylicium* LsrB, the amino acid sequence was truncated after residue 23 for all experiments. For *T. composti* LsrB, the program identified the cleavage site between amino acids 19 and 20. This truncation, Truncation 1, was used for subsequent purifications, bioassays, and crystallization trials.

However, after unsuccessful crystallization, four addition truncations of *T. composti* LsrB were determined from amino acid sequence alignments using protein Basic Local Alignment Search Tool (BLAST) and fold-recognition structural alignments (PHYRE^2) to test the hypothesis that the Truncation 1 construct is not crystallizing because of a disordered N-terminus. The subsequent truncations, denoted Truncation 2-5, have increasingly less conservative N-terminal deletions after amino acid residues Glu40, Pro43, Gln46, and Thr48, respectively (Supplemental Figure 2). These additional constructs are currently being generated through TOPO cloning.[34]

Mutagenesis of T. composti Active Site Residues

In the binding site of *T. composti* LsrB, four of the six residues are variant compared to *S. typhimurium* LsrB as follows: D166→N184, E167→L185, P220→N238, and A222→S240. Only the lysine (K54) and aspartate (D135) residues in the binding site of *T. composti* LsrB are conserved. Alanine mutants of the putative binding site residues were made using the QuikChange Lightning Site-Directed Mutagenesis Kit (Agilent). Primers were generated using the QuikChange Primer Design Program[35] and ordered from Sigma Aldrich. Sequencing of the PCR products (Genewiz) indicated that mutagenesis of the amino acids D135A, N184A, N238A, and S240A was successful. The K54A and L185A mutants were not successfully created with primers generated from the Primer Design program.

AI-2 Bioassay of the Putative T. composti and C. saccharobutylicium LsrB Receptors

The reporter strain *Vibrio harveyi* MM32 was used to detect levels of AI-2 in LuxS+ and LuxS- samples of several LsrB proteins, as described previously.[19] MM32 cells cannot produce endogenous AI-2 but still respond to exogenously supplied AI-2 through the detectable emission of light. Cell cultures were grown at 30°C in 5 mL of AB medium overnight (~15 hours) then diluted 1:5000 in fresh AB medium the next day.[36] Protein samples of LuxS+ *T. composti* and *C. saccharobutylicium* LsrB were denatured at 70°C and pelleted for 5 minutes at 14,000 rpm (Sorvall Legend RT+ Centrifuge, ThermoScientific). LuxS+ and LuxS- *B. cereus* LsrB samples were used as positive and negative controls, respectively. Additionally, a sample of Tris buffer (25 mM Tris, pH 8.0, 150 mM NaCl, 1 mM DTT) was used as a background control to correct for baseline fluorescence. In a 96-well black plate (Fisher Scientific), 10 µL of sample was added to 90 µL of diluted MM32 in triplicate. The plate was incubated at 30°C and continued shaking at 160 rpm for

the duration of the bioassay. Luminescence was measured as counts per seconds (CPS) with the Victor^2 (Wallac) luminometer every hour for 5 hours. The average fold induction (CPS/buffer) and standard deviation were calculated for each sample and reported for the bioluminescence.

Optimization of Protein Sample Preparation of the Alanine Mutants for the AI-2 Bioassay

The preliminary bioassay was conducted without any difficulty denaturing the LsrB samples. However, the D135A, N184A, N238A, and S240A mutants of *T. composti* LsrB did not denature under the same conditions. When the bioassay was conducted with each of the mutants, wild-type *T. composti* LsrB, and *B. cereus* controls, only the controls properly denatured after 3 minutes of heating at 70˚C. Alternate denaturing conditions were tested, including heating for 30 minutes at 100˚C, but the *T. composti* LsrB samples still did not denature completely. A small, gel-like pellet was observed for the wild-type protein, however, indicating some degree of unfolding. The alanine mutants, except for N184A, also showed partial denaturation after extreme heating with the formation of a very small white pellet after centrifugation. Current work probing alternative denaturing conditions, such as with guanadine hydrochloride[37] or non-specific proteases, is being conducted.

RESULTS

Previous work showing that murine gut bacteria belonging to the Firmicute phylum proliferate in response to AI-2 after dysbiosis[28] indicated that there are many bacteria that respond to the universal interspecies quorum sensing molecule that have yet to be identified and studied. Sequence alignments identified several LsrB orthologs from many bacterial species. We have since begun to investigate several potential LsrB receptors in bacteria belonging to the Firmicute

phylum, due to their sensitivity to AI-2[28]. We show through structural prediction models that *C. saccharobutylicium* and *T. composti*, two Firmicute bacteria identified in the query, have LsrB-like receptors with variant residues in the binding site. Furthermore, we confirm with a *Vibrio harveyi* bioassay that these wild-type orthologs bind AI-2 when grown in bacteria carrying LuxS. To determine which residues are essential for AI-2 binding, we have begun to assay the effect of alanine mutants in the binding pocket, which eliminate potential electrostatic and hydrogen bonding interactions between the protein and ligand.

Identification of LsrB Orthologs with Intermediate Sequence Identity

Since previous work identified functional receptors with sequence identity greater than 63% compared to *S. typhimurium* LsrB, we aimed to find additional functional orthologs with a lesser identity to previously-identified receptors to expand the repertoire of known functional LsrB receptors. We searched all completely sequenced genomes with the amino acid sequence of *Bacillus cereus* LsrB, a known AI-2 receptor belonging to the Firmicute phylum with 63% identity to *S. typhimurium* LsrB.[19] We used *B. cereus* LsrB to query all genomes because Firmicutes in the gut have been shown benefit from the presence of the signal molecule.[28] Thus, Firmicute bacteria are likely to have the LuxS synthase and contain functional *lsr* genes to encode for the LsrB receptor protein.[28] The bidirectional best-best hit algorithm yielded 890 results with sequence identities ranging from 30.0–49.6% as compared to *B. cereus* LsrB. From these initial hits, we narrowed our experimental focus to only LsrB orthologs from the Firmicutes.[28] The most conserved LsrB ortholog from the Firmicute bacterium, *C. saccharobutylicium*, has 39.5% identity with *B. cereus* LsrB and the least conserved LsrB, *T. composti*, has 30.1% identity. These two orthologs have 28% identity to each other (Supplemental Figure 3). Furthermore, the binding site

residues are only partially conserved. *C. saccharobutylicium* LsrB has two variant residues, while *T. composti* LsrB has four variant residues, which could potentially affect binding of AI-2.

Structural Predictions of T. composti and C. saccharobutylicium LsrB Orthologs

After determination by sequence alignment that *T. composti* and *C. saccharobutylicium* have LsrB-like receptors, we used fold-recognition software to model the three-dimensional structure of each putative LsrB receptor protein. We found that the main chain and side chains of several binding site residues are predicted to superimpose well onto *S. typhimurium* LsrB, despite variant amino acid composition (PDB: 1TJY) (Figure 2.1).

Furthermore, we modeled *R*-THMF in the binding site to determine potential hydrogen bonding interactions between the protein and ligand. In *S. typhimurium* LsrB, there are hydrogen bonding interactions between the ligand and the side chains of Lys35, Asp116, Asp166, and Gln167.[19] Moreover, Pro220 and Ala222 hydrogen bond with AI-2 through the main chain carbonyl and amine, respectively. In *T. composti* LsrB, residues Lys54 and Asp135 are positioned to be able to form hydrogen bonds with hydroxyl groups of *R*-THMF (Figure 2.1A). These putative hydrogen bonding interactions are conserved between *S. typhimurium* and *T. composti* LsrB, which could indicate that they are necessary for AI-2 recognition.

The four other predicted binding site residues in *T. composti* LsrB are variant, which could affect the hydrogen bonding and electrostatic interactions with AI-2. The variations of Asp166 to Gln184 and Gln167 to Leu185 in *T. composti* LsrB could prevent the formation of stabilizing hydrogen bonds to AI-2 either through the side chains or the main chain (Figure 2.1A). Residue Asn238 in

T. composti LsrB is positioned to interact with AI-2 through the backbone carbonyl, which would maintain the hydrogen bonding interactions at that residue. Moreover, the variation of Ala222 in *S. typhimurium* LsrB to Ser240 in *T. composti* LsrB has the potential to form a second hydrogen bond through the side chain at that position.

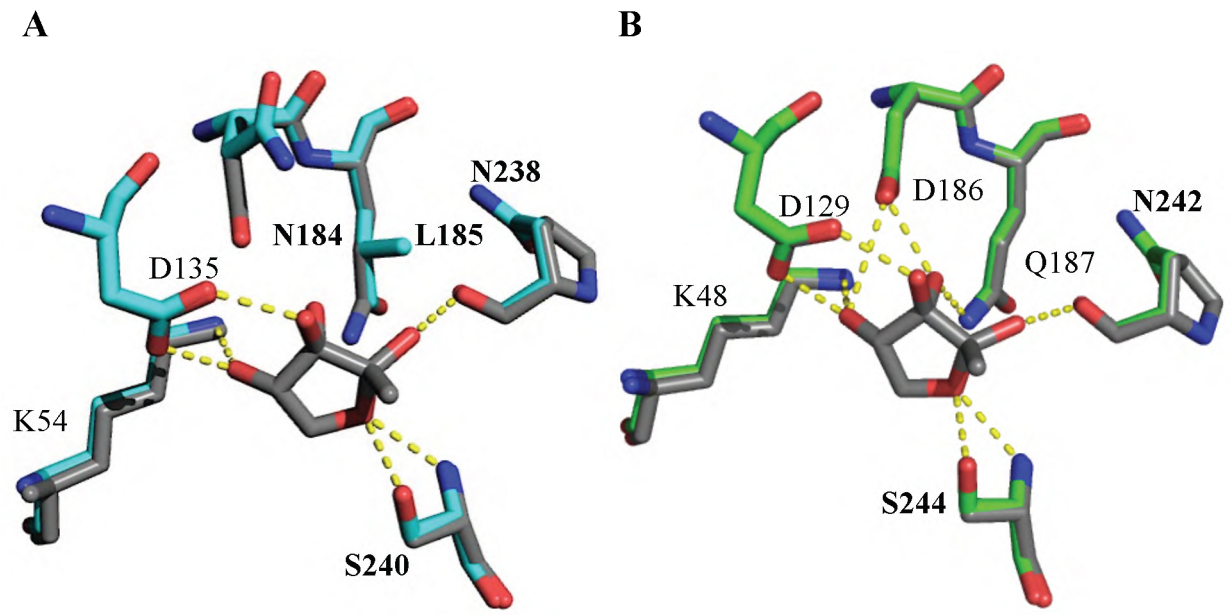

Figure 2.1 *Structural prediction alignments of the binding sites of (**A**) T. composti (cyan) and (**B**) C. saccharobutylicium (green) LsrB to S. typhimurium LsrB (grey) with AI-2 bound. Theoretical hydrogen bonds between the novel LsrB receptors and the AI-2 ligand are shown in yellow. Variant residues in the novel LsrB proteins are in bold.*

The binding pocket of *S. typhimurium* LsrB is charged due to two negatively charged aspartate residues (Asp116 and Asp166) and a positively charged lysine (Lys35).[19] A salt bridge forms between Lys35 and Asp166, giving a net negative charge to the binding site. By contrast, variation of the negatively charged Asp116 in *S. typhimurium* LsrB to Asn184 in the binding site of *T. composti* LsrB breaks the salt bridge, as the Lys54 and Asn135 residues of *T. composti* LsrB are

not predicted to be positioned to form a salt bridge. Furthermore, the pocket is predicted to have a net neutral charge. Thus, the electrostatic and hydrogen bonding interactions with the AI-2 ligand in the binding site of *T. composti* LsrB are predicted to be notably distinct from those in *S. typhimurium* LsrB.

A model of *C. saccharobutylicium* LsrB was also created to determine the putative interactions between the binding site residues and *R*-THMF (Figure 2.1B). In *C. saccharobutylicium* LsrB, only two binding site residues are variant, therefore the predicted binding pocket highly resembles that of *S. typhimurium* LsrB. The variation of Pro220 to Asn242 in *C. saccharobutylicium* LsrB potentially preserves the hydrogen bond through the main-chain carbonyl while the variation of Ala222 in *S. typhimurium* LsrB to Ser244 in *C. saccharobutylicium* LsrB is predicted to be positioned to form a second hydrogen bond through the side chain. The electrostatic interactions between Lys48 and Asp186 could form a salt bridge while the negatively charged Asp129 contributes to the net negative charge of the binding site, as in *S. typhimurium* LsrB.

Bioassay of Novel LsrB Orthologs

After identifying several bacteria with intermediate sequence identity to *B. cereus* LsrB and modeling the predicted binding site of each ortholog (Figure 2.1), we ran a bioassay using a *V. harveyi* reporter strain to determine if the orthologs are functional LsrB-like receptors.[38] The samples of the LsrB orthologs from *T. composti* and *C. saccharobutylicium* purified in LuxS+ strains of *E. coli* induced bioluminescence, indicating that they are AI-2 receptors (Figure 2.2). The bioassay was conducted with positive and negative controls of LuxS+ and LuxS- *B. cereus*

LsrB, respectively, to ensure that the measurement of light production was indicative of AI-2 binding to the *V. harveyi* AI-2 receptor.

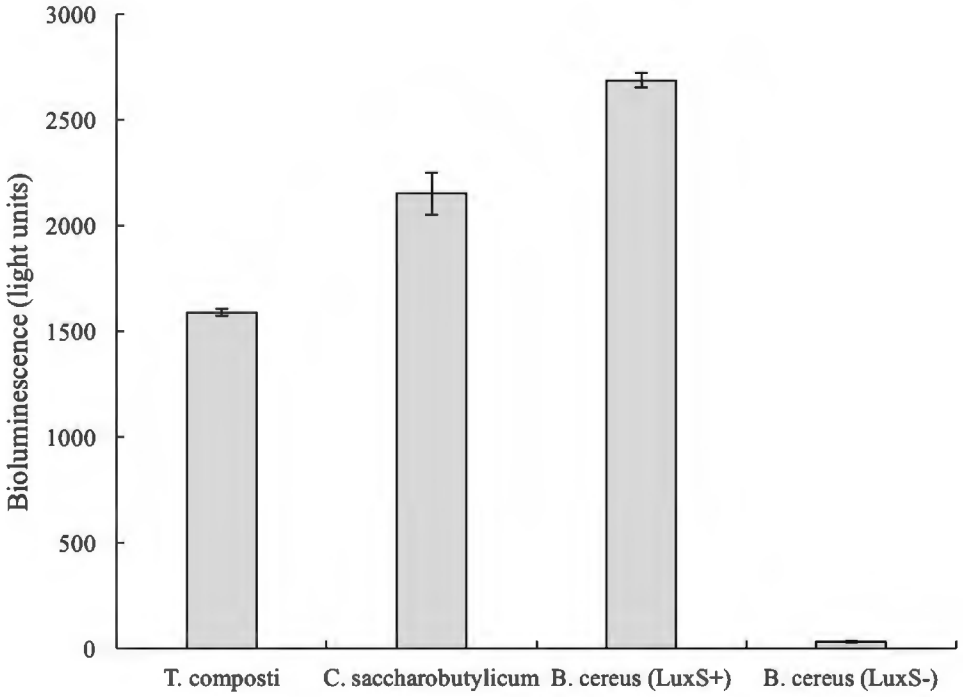

Figure 2.2 *Bioassay of the novel LsrB receptor proteins from LuxS+ T. composti and C. saccharobutylicium. The maximum light production, at 5 hours, is shown as a representative time point for the qualitative determination of AI-2 binding by the orthologs. The negative control, LuxS- B. cereus, shows that in the absence of the AI-2 synthase, the signal molecule is not produced and no light is emitted by the V. harveyi reporter. The LuxS+ B. cereus LsrB sample was used as positive control because it is a known AI-2 receptor. The samples containing the novel LsrB orthologs emit light, which indicates that they are functional AI-2 receptors.*

Comparison of the Solved Crystal Structure of C. saccharobutylicium LsrB to the Predicted Model and the Representative LsrB Receptor from S. typhimurium

C. saccharobutylicium LsrB was crystallized in 0.1 M citric acid, pH 2.75 and 26% PEG-3350 then cryoprotected in 27% PEG-3350 with 15% glycerol, yielding a crystal (space group: $P4_322$)

that diffracted to a final resolution of 1.35 Å after optimization (personal communication with Torcato, 2017). To assess the accuracy of our structural predictions, we aligned the solved structure of *C. saccharobutylicium* LsrB with the prediction model (Figure 2.3A). In the model, there are minor deviations from the observed structure, such as the direction of the serine hydroxyl group, but the alignment of the binding site residues shows that the prediction was very good (RMSD=0.201). Finally, we compared the binding sites of *C. saccharobutylicium* LsrB and *S. typhimurium* LsrB and observed that the residues form a similar binding pocket in both LsrB receptors (Figure 2.3B). The main differences between the two binding sites result from mutations of the amino acids that interact with AI-2 rather than the three-dimensional orientation of the residues in the binding pocket.

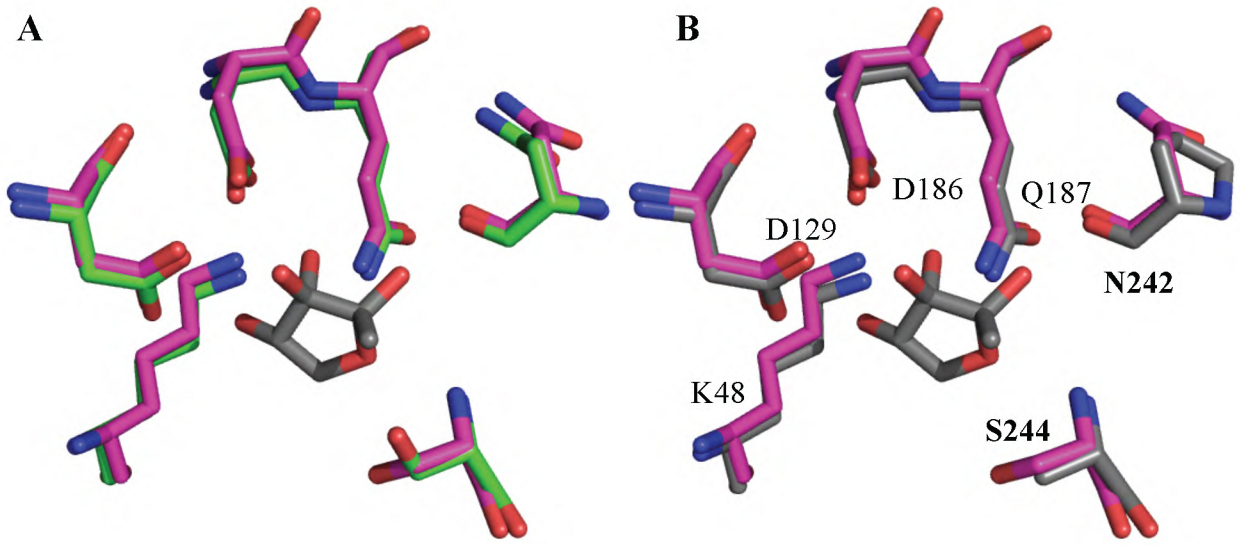

Figure 2.3 *Structural alignments of the solved crystal structure (pink) with the (**A**) predicted binding site of C. saccharobutylicium LsrB (green) and (**B**) S. typhimurium LsrB (grey). Mutated residues are bolded.*

DISCUSSION

Previous distinctions between groups of LsrB orthologs were limited to functional receptors with high sequence identity to *S. typhimurium* LsrB and non-quorum sensing proteins with low sequence identity. Recent investigation into additional LsrB orthologs revealed a third group of LsrB-like proteins that are functional AI-2 receptors and have intermediate sequence identity to the query, *B. cereus* LsrB. From the hundreds of hits that were identified in this search, we focused on Firmicute bacteria due to their responsiveness in the murine gut to exogenously produced AI-2 and their potential to have functional *lsr* genes.[28]

Structural alignments of *T. composti* and *C. saccharobutylicium* LsrB to *S. typhimurium* LsrB showed that the predicted binding site models closely resemble the known AI-2 receptor (Figure 2.1). However, from these models alone we could not confirm that these orthologs are functional LsrB receptors. We performed a bioassay that measures light production by *V. harveyi* cells, which cannot produce their own AI-2, to qualitatively analyze if there is binding of the ligand to the putative receptor proteins. The *V. harveyi* bioassay showed that both *T. composti* and *C. saccharobutylicium* LsrB demonstrate AI-2 binding activity in a LuxS-dependent manner, confirming that they are functional LsrB-like receptors (Figure 2.2). Thus, despite variations in the predicted binding site residues and an intermediate sequence identity to *B. cereus* LsrB, these receptors recognize AI-2.

To assay the importance of each residue in binding the AI-2 signal, we have constructed the mutants D135A, N184A, N238A, and S240A from *T. composti* LsrB. We aimed to perform the *V. harveyi* bioassay with these alanine mutants to investigate if they still bind AI-2, however, the

mutants did not denature under the typical conditions used for the bioassay (3 minutes heating at 70°C). After heating, there was no visible precipitant and no pellet formed after centrifuging. Thus, denaturation of the alanine mutants was attempted at 100°C for 30 minutes but the protein remained highly soluble and mostly folded. The folding and unfolding was monitored through measurements of the absorbance (NanoDrop) before and after heating. We found that after boiling for half an hour, the wild-type *T. composti* LsrB formed a gel-like pellet, but only about 10% of the protein denatured. The demonstrated stability of wild-type *T. composti* LsrB and alanine mutants of the receptor can be partially rationalized because the bacteria from which the proteins are derived is slightly thermophilic, as indicated by its genus *Thermobacillus*. We are currently investigating the hypothesis that the use of non-specific proteases will destabilize the protein and allow for use in denaturation of the *T. composti* samples for the bioassay.

The determination that the Firmicute bacteria *T. composti* and *C. saccharobutylicium* contain novel AI-2 receptors allowed us to pursue crystallization trials and binding affinity assays. We obtained a crystal structure for *C. saccharobutylicium* LsrB bound to *R*-THMF, which confirmed that the model prediction was accurate, giving credence to the model we generated for *T. composti* LsrB. We are currently working to verify the predicted structure of *T. composti* LsrB and to identify the form of AI-2 recognized by the receptor through crystallization trials (Chapter 5).

Furthermore, we investigating which residues are essential for the ligand-protein interaction by mutating each binding site residue to alanine and testing the bioassay activity of each. A bioassay of the mutant LsrB receptors should elucidate which binding site residues are essential for the uptake of AI-2 through the elimination of light production when the ligand can no longer bind the

receptor as a result of the mutation. In addition, ITC experiments on the wild-type and alanine mutants of the LsrB proteins are being conducted to determine the binding affinity of the receptor to AI-2 and the role of each residue in signal recognition (Chapter 4).

Chapter 3. Expression and Purification of *Thermobacillus composti* and *Clostridium saccharobutylicium* LsrB

The *lsr* operon encodes for the genes *lsrACDBFGE* which are involved in the uptake and processing of the interspecies quorum sensing signal molecule AI-2. The *lsrB* gene encodes for the periplasmic receptor protein that forms an ABC transporter complex with the proteins LsrA, LsrC, and LsrD (Figure 1.2). As cell density increases and AI-2 accumulates in the environment, LsrB binds the signal molecule which is internalized through the ABC transporter. The signal is subsequently processed by a series of proteins encoded for by the *lsr* operon, depleting the signal from the environment. The final products after signal degradation, DHAP and acetyl-CoA, are biologically important molecules in cellular processes such as glycolysis,[25] suggesting that the quenching of quorum sensing has a physiological function, as well as regulating community-wide behaviors.

By showing that ortholog LsrB receptors with less than 60% sequence identity to *B. cereus* LsrB bind AI-2, we have expanded the repertoire of known interspecies quorum sensing receptors. The iterative process of searching for LsrB receptors can be carried out using these novel receptors as query sequences, further describing the extent of AI-2 mediated quorum sensing. Moreover, low sequence identity and binding site variations could indicate that AI-2 is interacting with the receptor in a novel form or that the receptor itself differs from the *S. typhimurium* or *B. cereus* LsrB. In order to characterize the binding interaction, the protein must be successfully produced and isolated. The expression and purification of *T. composti* and *C. saccharobutylicium* LsrB constructs from *E. coli* cells that possess or lack the LuxS synthase are detailed for use in future studies.

Upon purification of the receptor proteins using an optimized protocol, binding assays and crystallization trials can be conducted. Though initial bioassays (Figure 2.2) qualitatively demonstrated that *T. composti* and *C. saccharobutylicium* LsrB bind AI-2 (Chapter 2), the specific affinity of each receptor to the ligand molecule is unknown. We can thus determine the binding affinity to AI-2 using isothermal titration calorimetry (ITC) with the highly-purified protein (Chapter 4). Furthermore, *T. composti* and *C. saccharobutylicium* LsrB have mutations in the binding site residues compared to *S. typhimurium* LsrB (Figure 2.1), suggesting that the protein-ligand interactions could be distinct. Through the use of X-ray crystallography, we can visualize the binding site of each receptor bound to AI-2 and compare the binding interactions with the previously-characterized *S. typhimurium* LsrB.

MATERIALS AND METHODS

Cloning, Growth, and Expression of N-terminal deleted lsrB

The truncations for *T. composti* and *C. saccharobutylicium* LsrB were determined from sequence (BLAST) and structure alignments (PHYRE[2]) to eliminate the disordered signal sequence from the periplasmic receptors. The N-terminal deleted (1–19, 1–40, 1–43, 1–46, and 1–48; 1–23) *lsrB* genes from *T. composti* and *C. saccharobutylicium* were cloned into the pENTR–TEV–D-TOPO entry vector (Gateway System, Life Technologies) and transferred into the pDEST527 plasmid (Gateway LR Clonease Kit, Life Technologies). The hexahistidine tag (6xHis) was incorporated into the vectors to facilitate purification by Ni-NTA affinity columns[39] and the tobacco etch virus (TEV) protease recognition site was included in the construct to enable separation of the protein from the 6xHis tag.[40] The pDEST527 vector was MiniPrepped (Qiagen) then transformed into DH5α Ca^{2+}-competent cells. Finally, the vectors were incorporated into *Escherichia coli* LuxS+

and LuxS- BL21 DE3 cells for inducible expression. Frozen stocks of each bacteria in 1:1 LB medium (Difco) and 50% glycerol (MP Biomedicals) were stored at -80˚C.

To express the cloned protein, *E. coli* BL21 cells containing pDEST-6xHis-*lsrB* were added to LB medium containing 1 $mg{\cdot}mL^{-1}$ ampicillin (GoldBio) and grown to saturation overnight (15–18 hours) at 37˚C with shaking at 160 rpm (Amerex Instruments Gyromax™ 747R). The overnight culture was diluted 1:100 in LB medium containing 1 $mg{\cdot}mL^{-1}$ ampicillin and grown until OD_{595}=0.3 at which point the temperature was reduced to 22˚C to increase protein solubility upon expression.[41] When the cell density was OD_{595}=0.9, expression of the vector was induced by the addition of 0.3 mM isopropyl-β-D-1-thiogalactopyranoside (IPTG; GoldBio). The cells continued to grow overnight (9–18 hours) and were harvested by centrifugation at 8000 rpm (ThermoScientific Sorvall Legend RT+ Centrifuge) for 12 minutes, resuspended in approximately 30 mL supernatant, then pelleted at 4000 rpm (ThermoScientific Sorvall RC 6+ Centrifuge) for 30 minutes and stored at -80˚C.

Purification of T. composti LsrB

Cell pellets were thawed on ice and resuspended in about 15 mL Lysis buffer (50 mM sodium phosphate, pH 8.0, 300 mM NaCl, 10 mM imidazole, 1.4 mM β-mercaptoethanol) per liter of original culture. The resuspended mixtures were also supplemented with 10 $\mu g{\cdot}mL^{-1}$ DNase I (Sigma), to cut DNA and improve lysate flow, and 10 $\mu g{\cdot}mL^{-1}$ leupeptin (CallBioChem), to inhibit protease degradation of the expressed protein. Resuspended cells were lysed using a M-110Y microfluidizer (Microfluidics) and the lysate was cleared by centrifugation at 16000 rpm (ThermoScientific Sorvall Legend RT+ Centrifuge) for 30 minutes.

Following lysis, 6xHis-LsrB was purified by nickel affinity chromatography. Three nickel nitrilotriacetic acid (Ni-NTA) agarose resin (Qiagen) columns (2 mL matrix) were preequilibrated in Lysis buffer and the lysate supernatant was passed over the columns in series. Five bed volumes of Wash buffer (50 mM sodium phosphate, pH 8.0, 300 mM NaCl, 20 mM imidazole, 1.4 mM β-mercaptoethanol) were run over the columns in parallel to remove nonspecifically bound impurities. Next, 6xHis-LsrB was eluted in 2 mL fractions from the columns in parallel with Elution buffer (50 mM sodium phosphate, pH 8.0, 300 mM NaCl, 250 mM imidazole, 1.4 mM β-mercaptoethanol). The protein content in each elution was quantified by UV-Vis absorbance[42] at 280 nm (Abs 0.1%=1.164 for *T. composti* 6xHis-LsrB, ExPASy ProtParam).[43] The protein purity of each elution was analyzed by SDS-PAGE.[44] The fractions containing 6xHis-LsrB were pooled and transferred into Tris buffer (25 mM Tris, pH 8.0, 150 mM NaCl, 1 mM DTT) using a Sephadex G25 column (GE Healthcare) to remove imidazole prior to TEV digestion.

The Ni-NTA purified protein was incubated with 1 mg TEV protease per 150 mg 6xHis-LsrB for a minimum of 18 hours at 4˚C to cleave the 6xHis tag. The digest mix was passed over two Ni-NTA columns in series preequilibrated in Tris buffer to separate the 6xHis tag and the TEV protease, which also contains a 6xHis fusion tag, from the cleaved LsrB. The columns were washed in parallel with two bed volumes of Wash buffer and fractions containing LsrB were pooled. The protein was transferred into Tris buffer (pH 7.0) and purified over Source 15Q ion exchange media (GE Healthcare) with a Tris buffer (pH 7.0) gradient of 50 mM to 400 mM NaCl over 30 column volumes. Finally, the protein was transferred into Tris buffer (pH 8.0) and purified with a HiLoad™ 16/60 Superdex™ 75 prep grade (M_r 3000–70000) column (Tricorn). The concentration

was quantified by UV-Vis absorbance at 280 nm (Abs 0.1%=1.221 for *T. composti* LsrB, ExPASy ProtParam) and the protein purity was analyzed by SDS-PAGE.

Purification of C. saccharobutylicium LsrB

The preparation of *C. saccharobutylicium* LsrB followed the purification protocol for *T. composti* LsrB with minor changes. The protein was incubated with 1 mg TEV protease per 300 mg 6xHis-LsrB (Abs 0.1%=1.510 for *C. saccharobutylicium* 6xHis-LsrB, ExPASy ProtParam) for a minimum of 12 hours. After elution from Ni-NTA columns, the LsrB (Abs 0.1%=1.530 for *C. saccharobutylicium* LsrB, ExPASy ProtParam) was swapped into Tris buffer (pH 8.0) and purified over Source 15Q ion exchange with a Tris buffer (pH 8.0) and gradient of 50 mM to 300 mM NaCl over 20 column volumes.

RESULTS

T. composti and *C. saccharobutylicium* LsrB were overexpressed and purified to maximize soluble protein and minimize impurities in the final solution. The purification of wild-type and alanine mutants of LsrB from both LuxS+ and LuxS- strains of *E. coli* was conducted with the same protocol.

Investigation of TEV protease digestion of T. composti 6xHis-LsrB

Hexahistidine (6xHis) tags that can be removed through protease activity have been developed to facilitate the purification of recombinant protein constructs with affinity and ion exchange chromatography.[39] Tobacco etch virus (TEV) protease is frequently used to cleave 6xHis or other fusion protein tags from the N-terminal domain of the purified protein of interest.[45] The removal

of tags from recombinant proteins can be necessary for the functioning and crystallization of the protein in its biologically relevant structure. Moreover, the efficiency of the protease is mediated by several variables including time and temperature of incubation as well as the ratio of protein to enzyme. In the determination of the purification protocol for *T. composti* LsrB, I investigated the effects of temperature, time of incubation, and concentration of TEV on the success of cutting and found that a 10-hour digest at 4˚C with 1 mg TEV per 300 mg protein was sufficient to cut most of the tag from 6xHis-LsrB (Figure 3.1). The TEV digest of *C. saccharobutylicium* LsrB was also conducted with these parameters and yielded efficient cutting (data not shown).

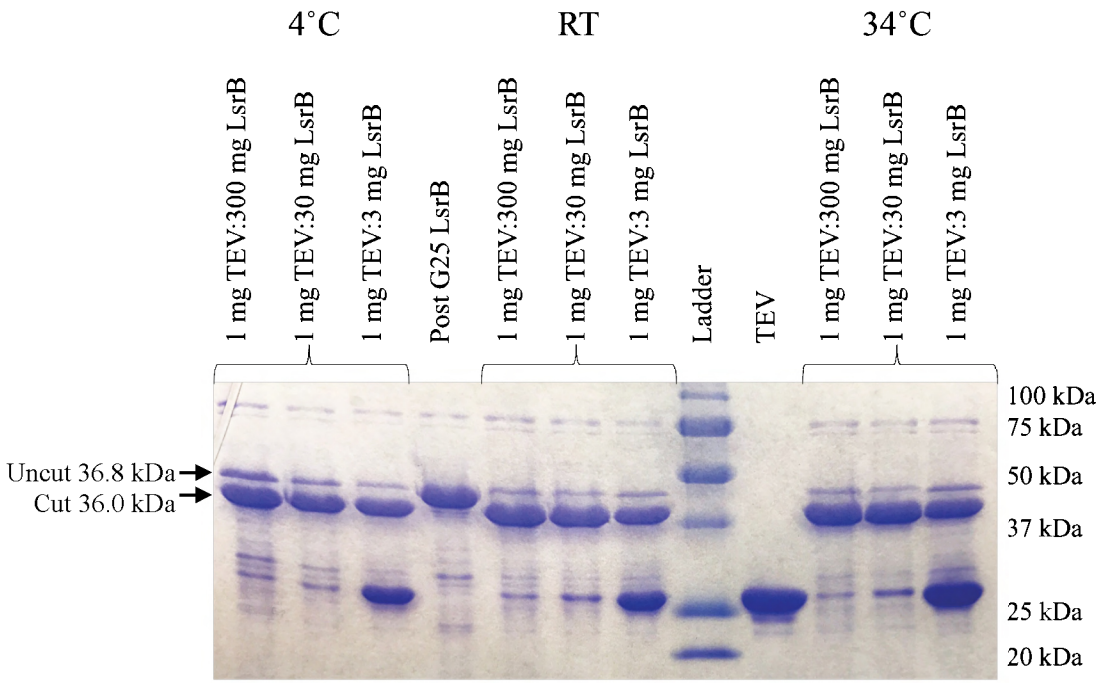

Figure 3.1 *SDS-PAGE analysis of TEV pilot study for a 10-hour digestion of T. composti LsrB in Tris buffer with varying proportions of TEV indicating that the 6xHis tag was sufficiently cleaved at 4˚C with a 1:300 mg ratio of TEV to LsrB. Uncut LsrB (Post G25 LsrB) has a molecular weight of 36.8 kDa and cut LsrB has a molecular weight of 36.0 kDa.*

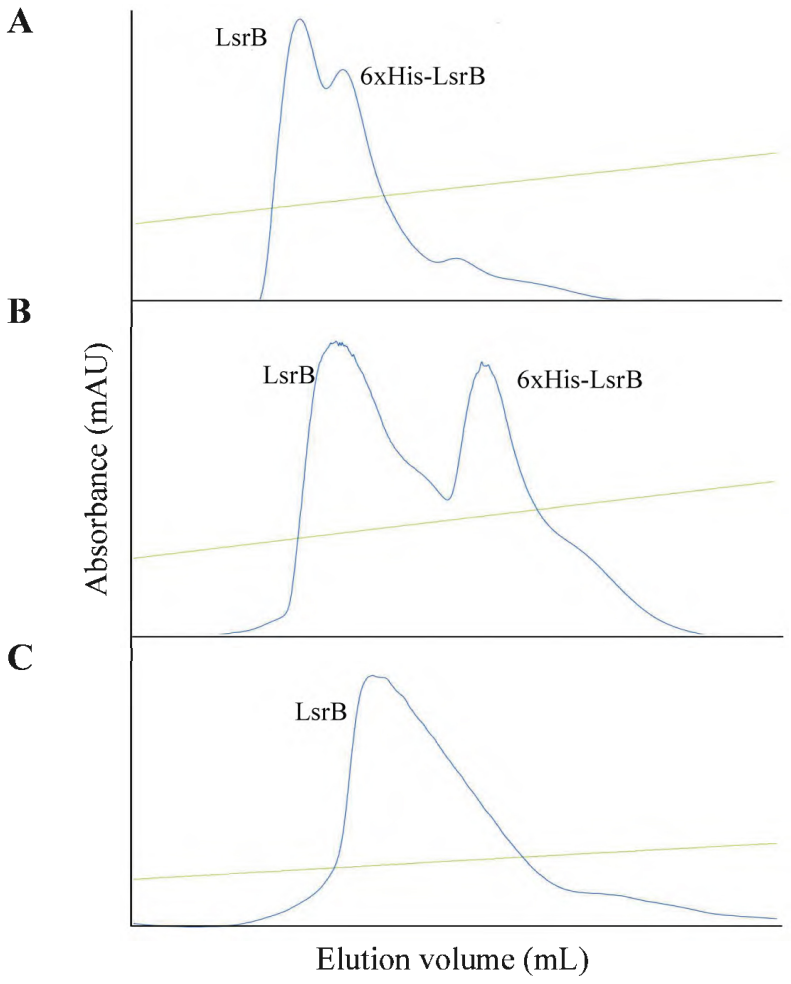

Figure 3.2 *Representative FPLC traces of anionic exchange chromatography separations of T. composti LsrB on (A) MonoQ resin at pH 8.0, (B) MonoQ resin at pH 7.0, and (C) Source 15Q resin at pH 7.0. Peaks are measured as absorbance units (mAU) at 280 nm. Green line represents the NaCl gradient.*

Optimization of Ion Exchange Purification of T. composti and C. saccharobutylicium LsrB

Following removal of the 6xHis tag and Ni-NTA purification, I determined the conditions required for ion exchange chromatography (IEC) purification of *T. composti* and *C. saccharobutylicium* LsrB. Initial trails of IEC were conducted on a MonoQ anionic exchange column in small quantities (less than 5 mg) with a 0 to 1 M NaCl gradient (GE Healthcare). The cut LsrB was

transferred into Tris buffer (50 mM NaCl) at pH 8.0 using Sephadex G25 gel filtration (GE Healthcare) and purified using the MonoQ. *T. composti* LsrB eluted from the column between 400-450 mM NaCl, but there was incomplete separation of cut and uncut (6xHis-LsrB) protein (Figure 3.2A). To optimize the purification, I transferred LsrB into Tris buffer (50 mM NaCl) at pH 7.0 instead, which resulted in better resolution of the cut and uncut LsrB peaks that were not separated in the Ni-NTA column compared to the pH 8.0 condition (Figure 3.2B). The IEC purification was scaled up on a Source 15Q anion exchange column (GE Healthcare) and yielded yet better separation of the cut and uncut LsrB species (Figure 3.2C; Supplemental Figure 4). The purification of *C. saccharobutylicium* LsrB was then optimized on the Source 15Q anion exchange column in Tris buffer (pH 8.0) giving clean separation of cut and uncut LsrB (data not shown).

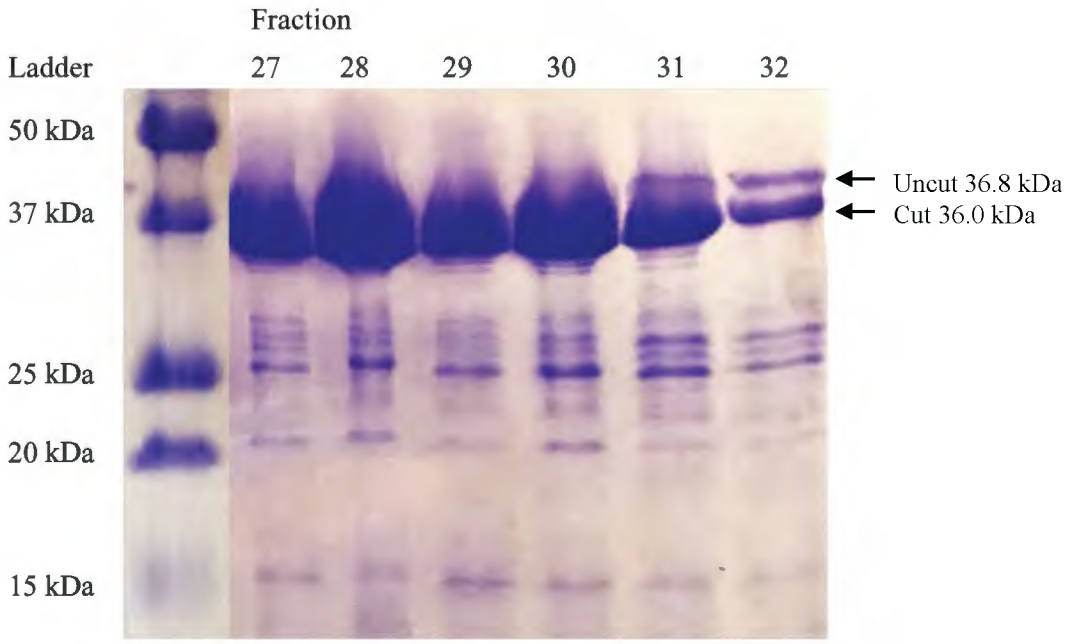

Figure 3.3 *SDS-PAGE analysis of T. composti LsrB eluted from IEC MonoQ column in Tris buffer (350-425 mM NaCl) at pH 7.0 showing separation between the cut and uncut LsrB between fractions 30 and 31.*

DISCUSSION

The periplasmic receptor protein, LsrB plays a crucial role in AI-2 mediated quorum sensing, thus we needed to optimize the purification for future assays and crystallization experiments. Furthermore, as we are investigating the properties of AI-2 binding to LsrB from a variety of species, we must determine appropriate purification protocols for each receptor.

The removal of the 6xHis tag from the recombinant protein after initial purification steps was optimized for *T. composti* and *C. saccharobutylicium* LsrB to use the minimum amount of protease with the shortest incubation time possible. Though previous work suggested using 1 mg TEV per 30 mg protein,[46,47] I determined that the use of one tenth the recommended amount of protease is sufficient for efficient removal of the 6xHis tag.

Furthermore, I found that by including an anionic exchange purification step to the previously described protocol[24] prior to size exclusion purification, I obtained even more pure protein to be used for crystallization trials. Though the two receptors described are orthologs of *S. typhimurium* LsrB, their surface interactions with the anionic resin are distinct as evidenced by the different pH conditions required for clean separation of contaminants from the desired protein product.

Chapter 4. Isothermal Titration Calorimetry of *Thermobacillus composti* and *Clostridium saccharobutylicium* LsrB

Interspecies AI-2-mediated quorum sensing is a cell density dependent process in which the small ligand molecule binds to the receptor protein, leading to internalization and processing of the signal and a coordinated communal response. We have identified LsrB orthologs in *T. composti* and *C. saccharobutylicium* LsrB that bind AI-2 and, as such, we are currently investigating the affinity with which each receptor bind the ligand. The equilibrium of the protein and ligand interaction is specified by the dissociation constant (K_D).

Determining the affinity of the LsrB-AI-2 interaction is essential for understanding the details of interspecies bacterial communication. Evolutionarily, bacteria might have evolved unique sensitivity to AI-2 depending on the threshold of ligand required to elicit a community-wide behavioral response. If the K_D is low, the ligand is more likely to be bound to the protein and, as such, the receptor has a higher affinity to the ligand. Moreover, the affinity of the ligand to the target receptor is dictated by electrostatic interactions, hydrogen bonding, and Van der Waals forces. Thus, variations in the binding site can affect the binding energy and equilibrium constant for the protein-ligand interaction. We hypothesized that each LsrB ortholog could have a distinct affinity to AI-2 due to variations in the binding interactions, leading to differential response rates to the signal molecule and, ultimately, to induce quorum sensing behavior.

The protein-ligand binding energetics can be directly measured through isothermal titration calorimetry (ITC), which monitors changes in the heat of reaction as the receptor presumably binds the ligand that is injected in small quantities into the protein solution.[48] Previous work has

quantified the LsrB-AI-2 interaction in *S. typhimurium* with an apparent K_D of about 160 μM using both ITC and a Fluorescence Resonance Energy Transfer (FRET) assay.[49] We propose here that the previously-reported K_D does not accurately reflect the LsrB-AI-2 affinity due to the imprecise methods used in the experiment to measure the concentration of DPD titrated into the protein solution.

Since identifying novel, functional LsrB receptors in a variety of bacterial species, we have begun to probe the binding affinity of AI-2 to each receptor to determine if separate species have evolved variable affinities to the ligand. For Firmicutes in the gut, a species-specific response to AI-2 could help maintain balanced bacterial levels, which is crucial for host health.[28] We are employing ITC to study the binding of AI-2 to several LsrB receptors including those of *T. composti* and *C. saccharobutylicium.*

MATERIALS AND METHODS

Preparation of stock solutions for ITC titrations

LsrB protein samples were produced in LuxS- *E. coli* cells and purified as described in Chapter 3. The anion exchange purification step was omitted, however, because we proposed that the Superdex™ 75 prep grade (M_r 3000–70000) column (Tricorn) yielded sufficient purification for the experiment.

Boron-free water, for AI-2 stock preparation, and ITC buffer were prepared using Amberlite IRA743 resin in batch mode (Darwish). The removal of boric acid and borate from water is necessary to ensure that most the AI-2 is present in the *R*-THMF conformation in solution. A stock

solution of *T. composti* LsrB was transferred into boron-free ITC buffer (25 mM sodium phosphate, pH 8.0, 150 mM NaCl, 1 mM β-mercaptoethanol) using Sephadex G25 gel filtration and prepared to a final concentration of 109.8 μM as verified by NMR. AI-2 for titration with *T. composti* LsrB was synthesized by the Ventura and Maycock labs (Instituto Gulbenkian de Ciência, Oeiras, Portugal)[50] and prepared to a final concentration of 3 mM. A stock solution of *C. saccharobutylicium* LsrB was prepared to a final concentration of 117.4 μM in boron-free ITC buffer and AI-2 for titration was prepared a final concentration of 800 μM in boron-free water. Both *T. composti* and *C. saccharobutylicium* LsrB solutions were dialyzed before titration to ensure that no artifacts from purification were bound to the receptor.

ITC measurements and calculations

ITC measurements were performed by Inês Torcato at the Instituto Gulbenkian de Ciência in Oeiras, Portugal in a MicroCal iTC200 microcalorimeter (GE Healthcare Biosciences) at 25°C. For the titration of *T. composti* LsrB, the reference power was set to 5 μcal/s and 19 injections of 2 μL AI-2 were added sequentially into 250 μL LsrB while stirring at 800 rpm. Identical conditions were used for AI-2 titration into ITC buffer to determine the heat of the dilution, which was included in the final calculations and analysis. The heat of reaction for each injection was calculated using MicroCal/Origin 7.0 software (GE Healthcare Biosciences) assuming a one-site binding model by integrating the area under each titration peak. For the titration of *C. saccharobutylicium* LsrB, 28 sequential injections of variable volumes of AI-2 were added into 250 μL LsrB while stirring as above. The titration of AI-2 into buffer was conducted at the same conditions to determine the heat of dilution, which was included in the final analysis as above.

RESULTS

We have begun to determine the binding constants of AI-2 to LsrB receptors from several bacterial species through ITC titrations. The apparent dissociation constant of AI-2 to *S. typhimurium* LsrB has been previously reported to be about 160 μM from FRET and ITC experiments, which indicates that the ligand is not tightly bound to the receptor.[49] The ITC experiments we are conducting will allow us to quantitatively compare the binding sites of functional LsrB orthologs and hypothesize how mutations in binding site residues affect binding to the receptor protein.

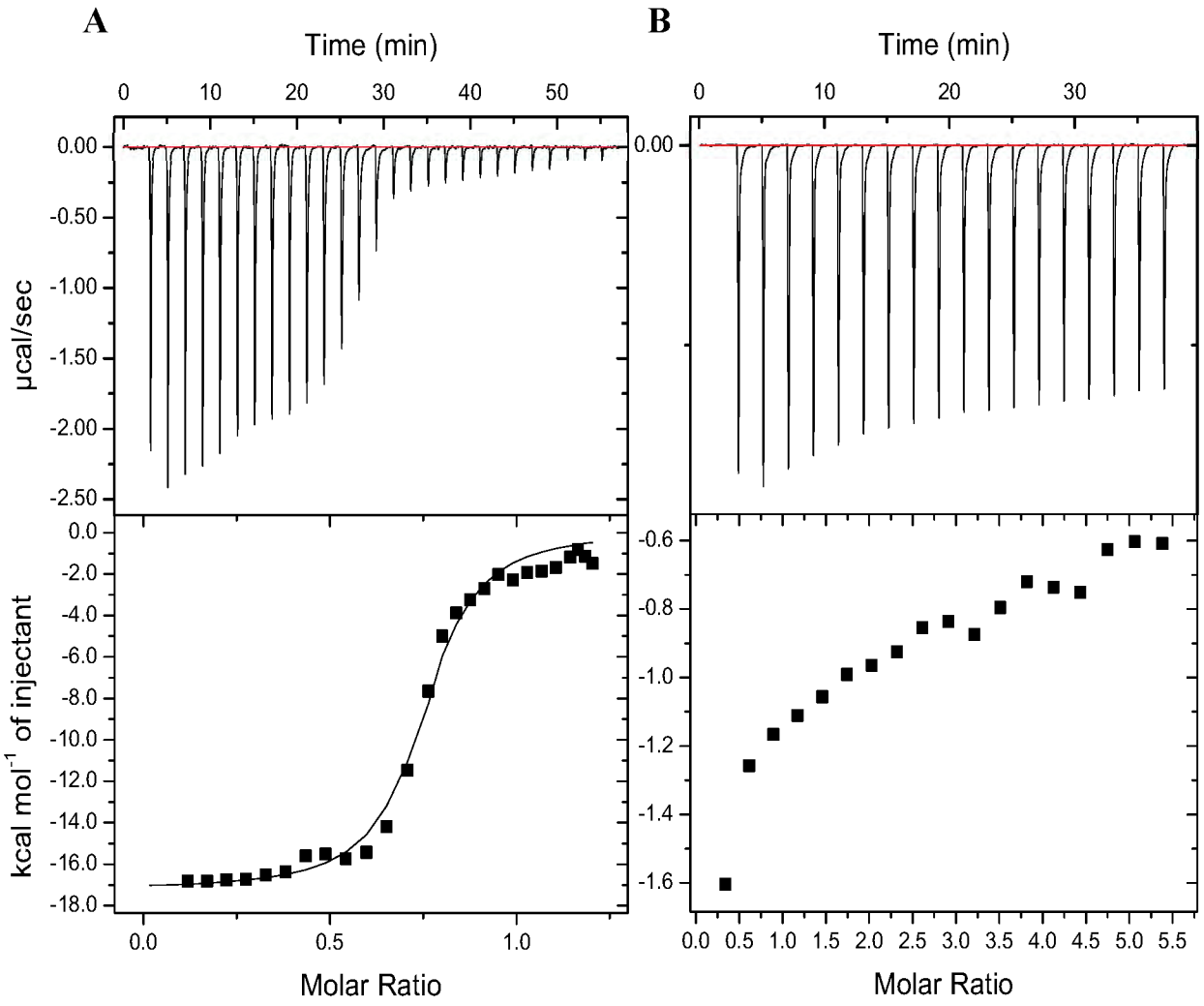

Figure 4.1 *ITC titrations of (**A**) C. saccharobutylicium and (**B**) T. composti LsrB with AI-2. The binding constant of C. saccharobutylicium LsrB was found to be 0.96±0.16 μM with an occupancy of 0.740±0.007. Titration of T. composti LsrB with AI-2 does not indicate binding.*

Determination of binding affinity of AI-2 to LsrB orthologs

After determination that the *C. saccharobutylicium* LsrB orthologs bind AI-2 (Figure 2.2), we aimed to quantify the binding affinity to compare the strength of interaction between related LsrB receptors. ITC titration of AI-2 with *C. saccharobutylicium* LsrB yielded a binding constant of approximately K_D=0.96±0.16 μM with an occupancy of 0.740±0.007 (Figure 4.1A). ITC titration of LsrB from *B. anthracis* measured an affinity four times higher than that of *C. saccharobutylicium* with a K_D=0.17 ± 0.03 μM and an occupancy of 0.881±0.004 (Supplemental Figure 5). Furthermore, despite previous determination that *T. composti* LsrB is a functional AI-2 receptor (Figure 2.2), ITC experiments did not show any binding event (Figure 4.1B) Increasing concentrations of AI-2 were added until the pure ligand itself was injected (7.26 mM) into the protein solution. Nevertheless, still no binding was observed for the ITC experiment with *T. composti* LsrB and AI-2.

DISCUSSION

By quantitatively measuring the affinity of the ligand to LsrB, we aim to elucidate differences in the protein-ligand interactions that result from amino acid variations in the binding sites of each receptor. We found that the binding of *C. saccharobutylicium* LsrB to AI-2 is four times weaker than the binding of *B. anthracis* LsrB to AI-2. To contextualize the binding affinity of AI-2 to the LsrB receptor protein, the K_D can be compared to similar types of ABC transporter complexes, like ribose binding protein (RBP). In *E. coli*, RBP is localized in the periplasm and binds ribose with a high affinity, given a K_D of about 0.13 μM as determined from equilibrium dialysis.[51] The data we obtained for LsrB has yielded K_D values in the same order of magnitude as the K_D for

RBP, which suggests that the ITC experiments we conducted are consistent with the behavior of similar protein structures and gives credence to the method we employed.

Previous work used both FRET and ITC to determine the affinity of AI-2 to *S. typhimurium* LsrB and obtained an apparent K_D of about 160 μM from both experiments, which suggests very poor binding.[49] Furthermore the observed K_D from the previous experiment is at least two orders of magnitude greater than the value we measured and the comparable value for the RBP-ribose binding interaction. The data for *S. typhimurium* LsrB binding to AI-2 was obtained using DPD produced from an enzymatic reaction between *S*-ribosylhomocysteine and a LuxS enzyme.[52] Quantification of the DPD concentration was done indirectly through measurement of the amount of homocysteine released, which does not factor for the amount of AI-2 available for binding to LsrB during the titration or other impurities in the titrant.[49]

Because AI-2 exists in an equilibrium between several forms of DPD (Figure 1.1), some of the ligand in solution cannot bind to the LsrB receptor, which has been shown to only recognize *R*-THMF. Thus, the indirect measurement of the AI-2 concentration leads to an overestimate of the amount of ligand that is binding in the ITC measurements with each injection, which increases the observed K_D. In the ITC experiments conducted for the novel LsrB receptors, we used DPD that was synthesized, characterized and quantified by NMR, and purified before titration.[50] Thus, we believe that the approach we employed to obtain the K_D for the AI-2-LsrB yields a more accurate reflection of the binding affinity than the value reported previously because of the direct method used to measure the concentration of AI-2 that was titrated with the protein.

The occupancy of the binding site for *C. saccharobutylicium* LsrB was lower than expected despite dialysis prior to titration to remove any bound artifacts. Ideally, the occupancy is equal to 1, indicating that 100% of the binding sites have complexed with ligand. These values are affected by the program fitting of the titration data and the concentrations of protein and AI-2 determined in the titrant and analyte solutions. However, the measured concentration of LsrB does not account for protein with artifacts still bound or misfolded proteins that cannot bind the ligand. Thus, the determined protein concentration could be an overestimate of the available binding sites, which lowers the observed occupancy. From the ITC titrations, we obtained about 74% occupancy for *C. saccharobutylicium* LsrB (Figure 4.1A) and 88% occupancy for *B. anthracis* LsrB (Supplemental Figure 5), which is high enough to be confident in the obtained K_D.

We decided to compare the affinity of AI-2 to different Firmicute bacteria to determine if there are differences in the K_D as a result of variations in the binding site. A smaller dissociation constant suggests that the ligand is internalized at smaller threshold concentrations of AI-2. Thus, from these ITC experiments we can posit that *B. anthracis* has a higher sensitivity for AI-2-mediated quorum sensing than does *C. saccharobutylicium*. To verify that the observed four-fold difference in K_D is functionally significant, replications and optimizations of the ITC experiments should be conducted to ensure that the concentrations of protein and ligand are accurately measured and to maximize the occupancy of the binding sites.

In the binding site of *C. saccharobutylicium* LsrB, four of the six residues are conserved (Figure 2.1), which, given the finding that it is less sensitive to AI-2, leads to the hypothesis that the two variable residues are contributing to the lower affinity of the LsrB ortholog to the ligand molecule.

To fully determine the stabilizing role of each residue in the binding site, ITC experiments on alanine mutants of *B. anthracis* and *C. saccharobutylicium* LsrB should be conducted. The mutant receptors could eliminate stabilizing hydrogen bonds between the binding site residues and the ligand molecule, affecting the binding affinity and elucidating the importance of each residue in the ligand-protein interaction.

The absence of AI-2 binding in the ITC titration with *T. composti* LsrB might indicate that some component that is essential for binding could be missing in the conditions of the experiment. A cofactor or another substance present in the binding site *in vivo* could be required for *T. composti* LsrB to recognize AI-2. In the case of AI-2-mediated quorum sensing in *Vibrio* species, boron is necessary for the recognition of the signal by the LuxP receptor.[19] The DPD equilibrium between the two known active forms of AI-2, *R*-THMF and *S*-THMF-borate, is mediated by the presence of boric acid (Figure 1.1). Thus, it is possible that another form of AI-2 that has yet to be identified is in equilibrium with another compound that is required for the signal to bind to the *T. composti* AI-2 receptor.

Alternatively, the interaction between AI-2 and *T. composti* LsrB could be thermodynamically undetectable, since ITC measures enthalpic changes upon binding of the ligand, in which case other methods of quantifying the binding affinity, such as fluorescence spectroscopy, could be explored. Future work on the *T. composti* receptor could also test AI-2 binding under conditions similar to those *in vivo* to determine if other factors are needed for recognition of AI-2. Furthermore, determination of the structure of *T. composti* LsrB through crystallization would elucidate the form of AI-2 bound to the receptor. Due to the number of variable residues in the

binding site, it is possible that the active form of AI-2 recognized by *T. composti* LsrB is not *R*-THMF and the receptor has a novel conformation that recognizes a novel adduct of AI-2. Further studies must be performed to determine the functionality and binding affinity of this protein.

Chapter 5. Attempted Crystallization of *Thermobacillus composti* LsrB

The enzyme LuxS produces the autoinducer signal 4,5-dihydroxy-2,3-pentanedione (DPD), which exists in an equilibrium between the linear form and a cyclized homocysteine ring.[19] In *S. typhimurium*, the LsrB receptor has been shown to bind a cyclized form of DPD known as (2R,4S)-2-methyl-2,3,3,4-tetrahydroxytetrahydrofuran (R-THMF).[19] The binding site of *S. typhimurium* LsrB contains six residues that are proposed to interact with R-THMF through hydrogen bonding, as determined from a crystal structure of the receptor with AI-2 bound.[19] The three charged residues Lys35, Asp116, and Asp166, as well as Gln167, hydrogen bond to the ligand through the side chain, whereas Pro220 and Ala222 hydrogen bond to R-TMHF through the backbone carbonyl and amine, respectively (Figures 3A and 3B).[19] A salt bridge forms between Lys35 and Asp166, leaving the pocket with a net negative charge, which is electrostatically stabilized by the hydrogen bonding interactions when AI-2 is bound.

In *T. composti* LsrB, four of the six binding site residues are variable, which could indicate that there are distinct protein-ligand interactions compared to the previously-described *holo* structures for *S. typhimurium*, *Yersinia pestis*, *Sinorhizobium meliloti* LsrB (PDB: 1TJY, 3T95, and 3EJW, respectively). Lys35 and Asp116 are conserved in the binding pocket of *T. composti* LsrB, which suggests that these residues are essential for AI-2 binding to the receptor. However, Asp166 and Pro220 are mutated to asparagine, Gln167 is mutated to lysine, and Ala222 is mutated to serine, which adds variability in the binding site of *T. composti* LsrB that could create a distinct binding pocket that accommodates a novel form of the AI-2 signal molecule from those previously described. Furthermore, these variations potentially eliminate the salt bridge formation and leave the pocket of *T. composti* LsrB with a net neutral charge. Thus, I aimed to crystallize *T. composti*

LsrB in the presence of AI-2 in order to visualize the orientation, identity, and form of the ligand bound and its interactions with the binding site residues.

MATERIALS AND METHODS

T. composti LsrB Truncation 1 Crystallization Attempts

The purification of *T. composti* LsrB was done from LuxS+ *E. coli* cells with the hopes observing AI-2 in the binding site. Pre-crystallization tests (PCT, Hampton Research) suggested a concentration for crystallization of *T. composti* LsrB of 40–60 mg·mL^{-1}. Crystallization screens were carried out primarily at room temperature via the hanging drop vapor diffusion method unless otherwise noted.

Initially, crystal Index™ screens (Hampton Research) were performed at lower concentrations of 10.0, 14.6, and 21.7 mg·mL^{-1} to sample the conditions without depleting the stock of purified protein. The screens at 10.0 and 14.6 mg·mL^{-1} were done via sitting drop method. After 24 hours, several wells with polyethylene glycol (PEG) conditions had phase separation (Supplemental Table 1). Thus, the PEGR$_X$™ (Hampton Research) screen was performed at 22.9, 38.1, and 63.4 mg·mL^{-1} and analysis of the well conditions suggested the use of the precipitant PEG-3350 in BIS-Tris, pH 5.5–7 in the presence of ammonium sulfate salt (Supplemental Tables 2 and 3).

Screens against concentration of ammonium sulfate (0.075–0.450 M), percent composition of PEG-3350 (22–27%), and pH of BIS-Tris (5.5–7.0) were performed at 38.3 and 61.5 mg·mL^{-1} at room temperature and at 46.2 mg·mL^{-1} at 4°C to slow the rate of diffusion. Significant phase separation was observed for several conditions at 25–27% PEG-3350 and 0.075–0.325 M $AmSO_4$.

An Additive Screen™ (Hampton Research) was done at 47.7 mg·mL^{-1} in 0.1 M BIS-Tris, pH 6.0, 0.1 M $AmSO_4$, and 25% PEG-3350 at 4˚C which yielded further phase separation and granular precipitate. The inability to crystallize Truncation 1 led to the creation of four additional truncations that removed N-terminal residues to potentially increase order in that region of the protein (Supplemental Figure 2).

RESULTS

Upon successful expression and purification of *T. composti* LsrB, several crystallization trials were conducted with the goal of deducing the specific binding pocket interactions with the AI-2 ligand molecule. Initially, fold prediction software (PHYRE^2) was used to make a preliminary model for the *T. composti* LsrB active site and identify the binding site residues. A recently-solved structure for *C. saccharobutylicium* LsrB, which has two variant binding site residues, shows that the protein-ligand interactions in the three-dimensional fold prediction model align with the structure solved from X-ray crystallography, giving credence to the model I generated for *T. composti* LsrB (personal communication with Inês Torcato, 2017). However, due to many unsuccessful attempts to crystallize *T. composti* LsrB, we hypothesized that the recombinant protein construct made initially (Truncation 1) did not adequately remove the signal sequence, leaving disordered residues on the N-terminus of the protein and preventing crystallization.

Crystallization screens of LuxS+ T. composti LsrB

The crystallization attempts of *T. composti* LsrB began by sampling several conditions with a 96-well Index™ (Hampton Research). The screen varies buffer, pH, salt, precipitant, and additives to broadly select conditions suitable for the production of crystals. An initial pre-crystallization test

(Hampton Research) suggested that a concentration of about 10 mg·mL^{-1} would be sufficient for the screen. From this index, done in sitting drop wells, I observed some granular precipitate in the well containing 0.2 M $MgCl_2 \cdot 6H_2O$, 0.1 M Tris, pH 8.5, and 25% w/v polyethylene glycol (PEG)-3350. However, most wells were clear, which suggested that the protein was not concentrated enough to effectively crystallize. A second sitting drop Index™ was set up at about 15 mg·mL^{-1}, but fewer than half of the conditions had liquid-liquid phase separation, precipitate, or crashed protein. As a result, a third Index™ was conducted at about 22 mg·mL^{-1} using the hanging drop vapor diffusion method to eliminate lint impurities during preparation. In the higher concentration index, wells containing 0.2 M $MgCl_2 \cdot 6H_2O$, 0.1 M buffer, pH 5.5–8.5, and 25% w/v PEG-3350 had various amounts of phase separation.

From the indexes, the precipitant PEG-3350 was identified to potentially be able to induce crystallization of LuxS+ *T. composti* LsrB (Supplemental Table 1). A screen that varied pH of 0.1 M Tris buffer from 7.5 to 9.0 and concentration of PEG-3350 from 20.5–28.0% was developed for a 24-well plate with LsrB at 17 mg·mL^{-1}. The well solutions also contained 0.2 M $MgCl_2 \cdot 6H_2O$. Between pH 8.5–9.0 and 23.5–26.5% PEG-3350, small and disperse phase separation drops were observed. However, since none of the conditions yielded crystals other PEG precipitants were sampled.

The PEGR_x™ (Hampton Research) screen was performed at about 23, 38, and 63 mg·mL^{-1} LsrB, revealing several potential crystallization conditions (Supplemental Tables 2 and 3). The PEG screen showed that conditions with BIS-Tris, pH 5.5–6.5 and various weights and concentrations of PEG had light phase separation and, as such, could produce crystals of *T. composti* LsrB. Based

off conditions from the collective Index™ and PEGR$_x$™ screens, a 24-well screen against concentration of ammonium sulfate (0.075–0.45 M) and amount of PEG-3350 (22–27%) in well solutions of 0.1 M BIS-Tris, pH 5.5 was designed with *T. composti* LsrB at 62 mg·mL^{-1}. From this screen, phase separation was observed in conditions with 25–27% PEG-3350 at all concentrations of ammonium sulfate. The observed liquid-liquid phase separation for 0.1 M BIS-Tris, pH 5.5, 0.2 M $AmSO_4$, and 27% PEG-3350 is representative of the several conditions that produced small, monodisperse drops (Figure 5.1). However, none of the conditions tested were able to produce crystals of LuxS+ *T. composti* LsrB.

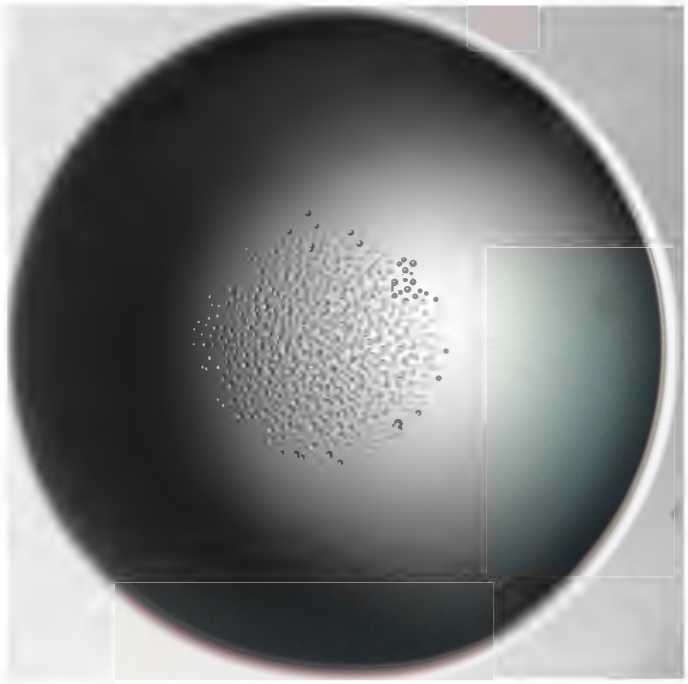

Figure 5.1 *Liquid-liquid phase separation of LuxS+ T. composti LsrB at 61.5 mg·mL^{-1} in 0.1 M BIS-Tris, pH 5.5, 0.2 M $AmSO_4$, and 27% PEG-3350. This representative image shows the small, disperse drops of phase separation obtained in several well conditions at various concentrations of LsrB.*

The condition of 0.1 M BIS-Tris, pH 6.0, 0.1 M $AmSO_4$, and 25% PEG-3350 was probed with an Additive Screen™ (Hampton Research) at about 48 $mg \cdot mL^{-1}$ LsrB to manipulate the solubility of *T. composti* LsrB and attempt to induce crystallization. Furthermore, this screen was conducted at 4°C with the hope of inducing crystallization from the slower rate of vapor diffusion in the protein drop. The addition of multivalent reagents to the drop caused the protein to crash out. Contrarily, the addition of salt, linker, polymer, carbohydrate, non-detergent, and organic reagents prevented the formation of liquid-liquid phase separation as was observed in the original condition tested. Detergent and amphiphile additives increased phase separation in the drop solution. The Additive Screen™ primarily eliminated possible reagents that would induce crystallization rather than elucidating additives that yielded LsrB crystals.

DISCUSSION

Despite unsuccessful attempts at crystallizing *T. composti* LsrB, the search parameters for potential crystallization conditions were narrowed down. After initial Index™ screens, conditions with PEG were focused on because the polymer is valuable during crystallization as a precipitant and functions as a cryoprotectant during freezing of crystals (Supplemental Table 1).[53] The $PEGR_x$™ screens indicate that alternative weight PEG solutions could yield crystals, including PEG-4000, PEG-6000, PEG monomethyl ether (PEG MME) 2000, and PEG MME 5000 (Supplemental Tables 2 and 3). Future crystallization studies on these precipitants could yield LsrB crystals. Furthermore, several conditions were eliminated from the Additive Screen™ that contained salt, linker, polymer, carbohydrate, non-detergent, organic, and multivalent additives and buffers at low pH.

There are several aspects of the crystallization process that can be optimized and probed in order to produce *T. composti* LsrB crystals. When setting up crystallization trials, many wells were contaminated by lint and other impurities in the drop solution. Subsequent screens should focus on obtaining highly pure LsrB through further optimization of the purification process, thus a revision of the purification protocol might be necessary. Moreover, because the LuxS+ *T. composti* LsrB was highly concentrated, there is a possibility that the binding site is not saturated with AI-2 if the affinity is not very strong, because the protein was washed with several volumes of buffer during the purification. Changes in the three-dimensional structures of the *holo* and *apo* forms of LsrB in the drop could lead to a non-homogenous solution of protein that cannot crystallize. Incubating LsrB with DPD in the appropriate drop conditions might homogenize the solution and yield crystals. Another way to induce crystallization is through seeding to introduce nucleation sites and produce larger, better-diffracting crystals.[54] However, crystals of *T. composti* LsrB have not been successfully produced, therefore another ortholog would have to be used.

Finally, the *T. composti* LsrB construct was determined from sequence alignments and three-dimensional structural predictions that indicated where the N-terminal signal sequence should be truncated. The construct that has been used for these crystallization trials has a conservative truncation of 19 amino acids (Supplemental Figure 1), but several additional constructs with larger truncations have been determined that remove more N-terminal residues (Supplemental Figure 2). These truncations were designed in an effort to eliminate disordered regions at the surface of the protein that are preventing crystallization. Future crystallization screens on these truncations might yield crystals with an ordered N-terminus that can pack into a crystal lattice more effectively.

Chapter 6. Conclusions and Future Directions

Since the discovery of AI-2-mediated quorum sensing in *Vibrio harveyi*,[13] several bacterial species have been shown to respond to the AI-2 signal both in the boronated[17] and non-boronated forms.[19,27] We have identified novel LsrB receptors from a variety of bacterial species and have begun to characterize AI-2 receptors from Firmicute bacteria, which have been previously shown to proliferate in the presence of exogenously produced AI-2.[28] We used sequence alignments to identify these orthologs and performed structural predictions to model the binding sites against a known LsrB receptor from *Salmonella typhimurium*.

From a *V. harveyi* bioassay, we determined that the *Thermobacillus composti* and *Clostridium saccharobutylicium* LsrB orthologs, which have 30.1% and 39.5% sequence identity with *Bacillus cereus* LsrB, respectively, are functional AI-2 receptors (Figure 2.2). We showed that despite the low sequence identity and variations in the binding site residues, these receptors bind AI-2. In identifying novel receptors, we hope to iteratively search for additional LsrB orthologs with yet lower sequence identity with the original query, *S. typhimurium* LsrB. By doing this, we are expanding the repertoire of known LsrB receptors, and as such, can characterize the binding interactions specific to each ortholog. We theorize that a novel form of AI-2 could be recognized by bacteria whose receptors are highly divergent from known LsrB receptors.

To quantitatively assess the effect of variations of the binding site residues in the binding affinity to AI-2, we have begun to run ITC experiments on several LsrB orthologs, including those from *B. cereus*, *C. saccharobutylicium*, and *T. composti*. Through ITC, we determined the K_D of *B. cereus* LsrB to be about 0.17 μM (Supplemental Figure 5) and the K_D of *C. saccharobutylicium* to

be about 0.96 μM (Figure 4.1A). The ITC experiment with *T. composti* LsrB did not show any binding interaction with DPD, despite finding in the bioassay that *T. composti* LsrB was bound to AI-2 in a LuxS-dependent manner (Figure 2.2). We have hypothesized that *T. composti* LsrB could have an artifact bound tightly to the receptor, preventing the binding of exogenously added AI-2. We have also theorized that the signal molecule recognized by the *T. composti* AI-2 receptor is a novel adduct that requires another cofactor or substance that is not present in the ITC experiment to be recognized by the LsrB ortholog. Because the *T. composti* LsrB binding pocket has variable amino acid residues at four of six residues, it is possible that the receptor recognizes an unidentified, novel adduct of the AI-2 signal molecule.

In order to fully characterize the ligand that is bound to the *T. composti* LsrB receptor and the hydrogen bonding and electrostatic interactions between the protein and ligand, we are working to crystallize the receptor with AI-2 bound. Crystallization attempts have yielded drops with liquid-liquid phase separation or precipitate at very high concentrations of protein, which indicates that the *T. composti* LsrB receptor could crystallize with an optimization of conditions. We proposed that the N-terminal region could be disordered due to incomplete removal of the signal peptide sequence and is, thus, preventing crystallization. As such, we are creating several additional N-terminal deleted constructions that will be purified and indexed for crystal growth. We obtained a crystal structure of *C. saccharobutylicium* LsrB that superimposes well onto the binding site of *S. typhimurium* LsrB (RMSD=0.201), which suggests that our predicted model for *T. composti* LsrB is valid.

The study of the interaction of the AI-2 signal molecule to the LsrB receptor from several species could elucidate an evolutionarily driven differential response rate to the signal molecule. The preliminary findings that *B. cereus* and *C. saccharobutylicium* have different affinities to the ligand suggest that bacteria have evolved different sensitivities to AI-2 based on the variations in the binding site residues. We aim to assay the effect of each binding site residue on the LsrB-AI-2 interaction by mutating each residue and conducting bioassays and ITC experiments that should indicate differences in binding ability and affinity.

By studying the specifics of AI-2 recognition by several LsrB orthologs through ITC and crystallization experiments, we aim to further characterize the form of the signal recognized and the sensitivity of each receptor to the signal molecule. With a better understanding of the interspecies quorum sensing circuit, we could potentially manipulate bacterial levels in conjunction with or in place of antibiotics to treat infections without the unintentional creation of antibiotic-resistant bacterial strains. Thus, the study of quorum sensing furthers our understanding of how bacteria communicate to coordinate community wide behaviors and presents a potential means of interference with the signaling mechanism to benefit human health.

Literature Cited

(1) Nealson, K. H.; Platt, T.; Hastings, J. W. Cellular Control of the Synthesis and Activity of the Bacterial Luminescent System. *J. Bacteriol.* **1970**, *104* (1), 313–322.

(2) Nealson, K. H.; Hastings, J. W. Bacterial Bioluminescence: Its Control and Ecological Significance. *Microbiol. Rev.* **1979**, *43* (4), 496–518.

(3) Ruby, E. G.; McFall-Ngai, M. J. A Squid That Glows in the Night: Development of an Animal-Bacterial Mutualism. *J. Bacteriol.* **1992**, *174* (15), 4865–4870.

(4) Miyamoto, C. M.; Boylan, M.; Graham, A. F.; Meighen, E. A. Organization of the Lux Structural Genes of Vibrio Harveyi. Expression under the T7 Bacteriophage Promoter, mRNA Analysis, and Nucleotide Sequence of the luxD Gene. *J. Biol. Chem.* **1988**, *263* (26), 13393–13399.

(5) Engebrecht, J.; Silverman, M. Identification of Genes and Gene Products Necessary for Bacterial Bioluminescence. *Proc. Natl. Acad. Sci. U. S. A.* **1984**, *81* (13), 4154–4158.

(6) Meighen, E. A. Molecular Biology of Bacterial Bioluminescence. *Microbiol. Rev.* **1991**, *55* (1), 123–142.

(7) Passador, L.; Cook, J. M.; Gambello, M. J.; Rust, L.; Iglewski, B. H. Expression of Pseudomonas Aeruginosa Virulence Genes Requires Cell-to-Cell Communication. *Science* **1993**, *260* (5111), 1127–1130.

(8) Costerton, J. W.; Lewandowski, Z.; Caldwell, D. E.; Korber, D. R.; Lappin-Scott, H. M. Microbial Biofilms. *Annu. Rev. Microbiol.* **1995**, *49*, 711–745.

(9) Pierson, L. S.; Keppenne, V. D.; Wood, D. W. Phenazine Antibiotic Biosynthesis in Pseudomonas Aureofaciens 30-84 Is Regulated by PhzR in Response to Cell Density. *J. Bacteriol.* **1994**, *176* (13), 3966–3974.

(10) Miller, M. B.; Bassler, B. L. Quorum Sensing in Bacteria. *Annu. Rev. Microbiol.* **2001**, *55*, 165–199.

(11) Engebrecht, J.; Nealson, K.; Silverman, M. Bacterial Bioluminescence: Isolation and Genetic Analysis of Functions from Vibrio Fischeri. *Cell* **1983**, *32* (3), 773–781.

(12) Kleerebezem, M.; Quadri, L. E.; Kuipers, O. P.; de Vos, W. M. Quorum Sensing by Peptide Pheromones and Two-Component Signal-Transduction Systems in Gram-Positive Bacteria. *Mol. Microbiol.* **1997**, *24* (5), 895–904.

(13) Federle, M. J. Autoinducer-2-Based Chemical Communication in Bacteria: Complexities of Interspecies Signaling. *Contrib. Microbiol.* **2009**, *16*, 18–32.

(14) Chen, X.; Schauder, S.; Potier, N.; Van Dorsselaer, A.; Pelczer, I.; Bassler, B. L.; Hughson, F. M. Structural Identification of a Bacterial Quorum-Sensing Signal Containing Boron. *Nature* **2002**, *415* (6871), 545–549.

(15) Surette, M. G.; Miller, M. B.; Bassler, B. L. Quorum Sensing in Escherichia Coli, Salmonella Typhimurium, and Vibrio Harveyi: A New Family of Genes Responsible for Autoinducer Production. *Proc. Natl. Acad. Sci. U. S. A.* **1999**, *96* (4), 1639–1644.

(16) Bassler, B. L. How Bacteria Talk to Each Other: Regulation of Gene Expression by Quorum Sensing. *Curr. Opin. Microbiol.* **1999**, *2* (6), 582–587.
(17) Bassler, B. L.; Wright, M.; Silverman, M. R. Multiple Signalling Systems Controlling Expression of Luminescence in Vibrio Harveyi: Sequence and Function of Genes Encoding a Second Sensory Pathway. *Mol. Microbiol.* **1994**, *13* (2), 273–286.
(18) Bassler, B. L.; Greenberg, E. P.; Stevens, A. M. Cross-Species Induction of Luminescence in the Quorum-Sensing Bacterium Vibrio Harveyi. *J. Bacteriol.* **1997**, *179* (12), 4043–4045.
(19) Miller, S. T.; Xavier, K. B.; Campagna, S. R.; Taga, M. E.; Semmelhack, M. F.; Bassler, B. L.; Hughson, F. M. Salmonella Typhimurium Recognizes a Chemically Distinct Form of the Bacterial Quorum-Sensing Signal AI-2. *Mol. Cell* **2004**, *15* (5), 677–687.
(20) A Handbook of Methods for the Analysis of Carbon Dioxide Parameters in Sea Water http://cdiac.ornl.gov/oceans/handbook.html (accessed Mar 27, 2017).
(21) Woods, W. G. An Introduction to Boron: History, Sources, Uses, and Chemistry. *Environ. Health Perspect.* **1994**, *102* (Suppl 7), 5–11.
(22) Xavier, K. B.; Miller, S. T.; Lu, W.; Kim, J. H.; Rabinowitz, J.; Pelczer, I.; Semmelhack, M. F.; Bassler, B. L. Phosphorylation and Processing of the Quorum-Sensing Molecule Autoinducer-2 in Enteric Bacteria. *ACS Chem. Biol.* **2007**, *2* (2), 128–136.
(23) Xavier, K. B.; Bassler, B. L. Regulation of Uptake and Processing of the Quorum-Sensing Autoinducer AI-2 in Escherichia Coli. *J. Bacteriol.* **2005**, *187* (1), 238–248.
(24) Marques, J. C.; Lamosa, P.; Russell, C.; Ventura, R.; Maycock, C.; Semmelhack, M. F.; Miller, S. T.; Xavier, K. B. Processing the Interspecies Quorum-Sensing Signal Autoinducer-2 (AI-2) CHARACTERIZATION OF PHOSPHO-(S)-4,5-DIHYDROXY-2,3-PENTANEDIONE ISOMERIZATION BY LsrG PROTEIN. *J. Biol. Chem.* **2011**, *286* (20), 18331–18343.
(25) Marques, J. C.; Oh, I. K.; Ly, D. C.; Lamosa, P.; Ventura, M. R.; Miller, S. T.; Xavier, K. B. LsrF, a Coenzyme A-Dependent Thiolase, Catalyzes the Terminal Step in Processing the Quorum Sensing Signal Autoinducer-2. *Proc. Natl. Acad. Sci. U. S. A.* **2014**, *111* (39), 14235–14240.
(26) Roy, V.; Fernandes, R.; Tsao, C.-Y.; Bentley, W. E. Cross Species Quorum Quenching Using a Native AI-2 Processing Enzyme. *ACS Chem. Biol.* **2010**, *5* (2), 223–232.
(27) Pereira, C. S.; de Regt, A. K.; Brito, P. H.; Miller, S. T.; Xavier, K. B. Identification of Functional LsrB-like Autoinducer-2 Receptors. *J. Bacteriol.* **2009**, *191* (22), 6975–6987.
(28) Thompson, J. A.; Oliveira, R. A.; Djukovic, A.; Ubeda, C.; Xavier, K. B. Manipulation of the Quorum Sensing Signal AI-2 Affects the Antibiotic-Treated Gut Microbiota. *Cell Rep.* **2015**, *10* (11), 1861–1871.
(29) Kelley, L. A.; Mezulis, S.; Yates, C. M.; Wass, M. N.; Sternberg, M. J. E. The Phyre2 Web Portal for Protein Modeling, Prediction and Analysis. *Nat. Protoc.* **2015**, *10* (6), 845–858.
(30) Sato, Y.; Nakaya, A.; Shiraishi, K.; Kawashima, S.; Goto, S.; Kanehisa, M. SSDB: Sequence Similarity Database in KEGG. *Genome Inform.* **2001**, *12*, 230–231.

(31) Kanehisa, M.; Goto, S. KEGG: Kyoto Encyclopedia of Genes and Genomes. *Nucleic Acids Res.* **2000**, *28* (1), 27–30.
(32) Marston, F. A. The Purification of Eukaryotic Polypeptides Synthesized in Escherichia Coli. *Biochem. J.* **1986**, *240* (1), 1–12.
(33) Petersen, T. N.; Brunak, S.; von Heijne, G.; Nielsen, H. SignalP 4.0: Discriminating Signal Peptides from Transmembrane Regions. *Nat. Methods* **2011**, *8* (10), 785–786.
(34) Wood, D. W.; Hsii, J.; Oak, S.; Contreras, L.; Chestnut, J. *Self-Cleaving Affinity Tags and Methods of Use*; Google Patents, 2005.
(35) Novoradovsky, A.; Zhang, (Vivian), V.; Ghosh, M.; Hogrefe, H.; Sorge, J. A.; Gaasterland, T. Computational Principles of Primer Design for Site Directed Mutagenesis. In *Computational Principles of Primer Design for Site Directed Mutagenesis*; Anaheim, CA, 2005; Vol. 1, pp 532–535.
(36) Kim, W.; Surette, M. G. Coordinated Regulation of Two Independent Cell-Cell Signaling Systems and Swarmer Differentiation in Salmonella Enterica Serovar Typhimurium. *J. Bacteriol.* **2006**, *188* (2), 431–440.
(37) Monera, O. D.; Kay, C. M.; Hodges, R. S. Protein Denaturation with Guanidine Hydrochloride or Urea Provides a Different Estimate of Stability Depending on the Contributions of Electrostatic Interactions. *Protein Sci. Publ. Protein Soc.* **1994**, *3* (11), 1984–1991.
(38) Taga, M. E.; Xavier, K. B. Methods for Analysis of Bacterial Autoinducer-2 Production. *Curr. Protoc. Microbiol.* **2011**, *Chapter 1*, Unit1C.1.
(39) Zhao, X.; Li, G.; Liang, S. Several Affinity Tags Commonly Used in Chromatographic Purification. *J. Anal. Methods Chem.* **2013**, *2013*, e581093.
(40) Lucast, L. J.; Batey, R. T.; Doudna, J. A. Large-Scale Purification of a Stable Form of Recombinant Tobacco Etch Virus Protease. *BioTechniques* **2001**, *30* (3), 544–546, 548, 550 passim.
(41) Sørensen, H. P.; Mortensen, K. K. Soluble Expression of Recombinant Proteins in the Cytoplasm of Escherichia Coli. *Microb. Cell Factories* **2005**, *4*, 1.
(42) Aitken, A.; Learmonth, M. P. Protein Determination by UV Absorption. In *The Protein Protocols Handbook*; Walker, J. M., Ed.; Humana Press: Totowa, NJ, 2009; pp 3–6.
(43) Artimo, P.; Jonnalagedda, M.; Arnold, K.; Baratin, D.; Csardi, G.; de Castro, E.; Duvaud, S.; Flegel, V.; Fortier, A.; Gasteiger, E.; et al. ExPASy: SIB Bioinformatics Resource Portal. *Nucleic Acids Res.* **2012**, *40* (Web Server issue), W597-603.
(44) Shapiro, A. L.; Viñuela, E.; Maizel, J. V. Molecular Weight Estimation of Polypeptide Chains by Electrophoresis in SDS-Polyacrylamide Gels. *Biochem. Biophys. Res. Commun.* **1967**, *28* (5), 815–820.
(45) Waugh, D. S. An Overview of Enzymatic Reagents for the Removal of Affinity Tags. *Protein Expr. Purif.* **2011**, *80* (2), 283–293.
(46) Hua, J. Studies on Two Putative AI-2 Receptors and the Transcriptional Repressor LsrR, Swarthmore College: Swarthmore, PA, 2015.

(47) Gale, E. Studies on the Transcriptional Repressor LsrR and Its Potential Interaction with DHAP, Swarthmore College: Swarthmore, PA, 2016.
(48) Leavitt, S.; Freire, E. Direct Measurement of Protein Binding Energetics by Isothermal Titration Calorimetry. *Curr. Opin. Struct. Biol.* **2001**, *11* (5), 560–566.
(49) Zhu, J.; Pei, D. A LuxP-Based Fluorescent Sensor for Bacterial Autoinducer II. *ACS Chem. Biol.* **2008**, *3* (2), 110–119.
(50) Ascenso, O. S.; Marques, J. C.; Santos, A. R.; Xavier, K. B.; Ventura, M. R.; Maycock, C. D. An Efficient Synthesis of the Precursor of AI-2, the Signalling Molecule for Inter-Species Quorum Sensing. *Bioorg. Med. Chem.* **2011**, *19* (3), 1236–1241.
(51) Binnie, R. A.; Zhang, H.; Mowbray, S.; Hermodson, M. A. Functional Mapping of the Surface of Escherichia Coli Ribose-Binding Protein: Mutations That Affect Chemotaxis and Transport. *Protein Sci. Publ. Protein Soc.* **1992**, *1* (12), 1642–1651.
(52) Rajamani, S.; Zhu, J.; Pei, D.; Sayre, R. A LuxP-FRET-Based Reporter for the Detection and Quantification of AI-2 Bacterial Quorum-Sensing Signal Compounds. *Biochemistry (Mosc.)* **2007**, *46* (13), 3990–3997.
(53) Berejnov, V.; Husseini, N. S.; Alsaied, O. A.; Thorne, R. E. Effects of Cryoprotectant Concentration and Cooling Rate on Vitrification of Aqueous Solutions. *J. Appl. Crystallogr.* **2006**, *39* (2), 244–251.
(54) Bergfors, T. Seeds to Crystals. *J. Struct. Biol.* **2003**, *142* (1), 66–76.

Supplemental Information

>Sequence

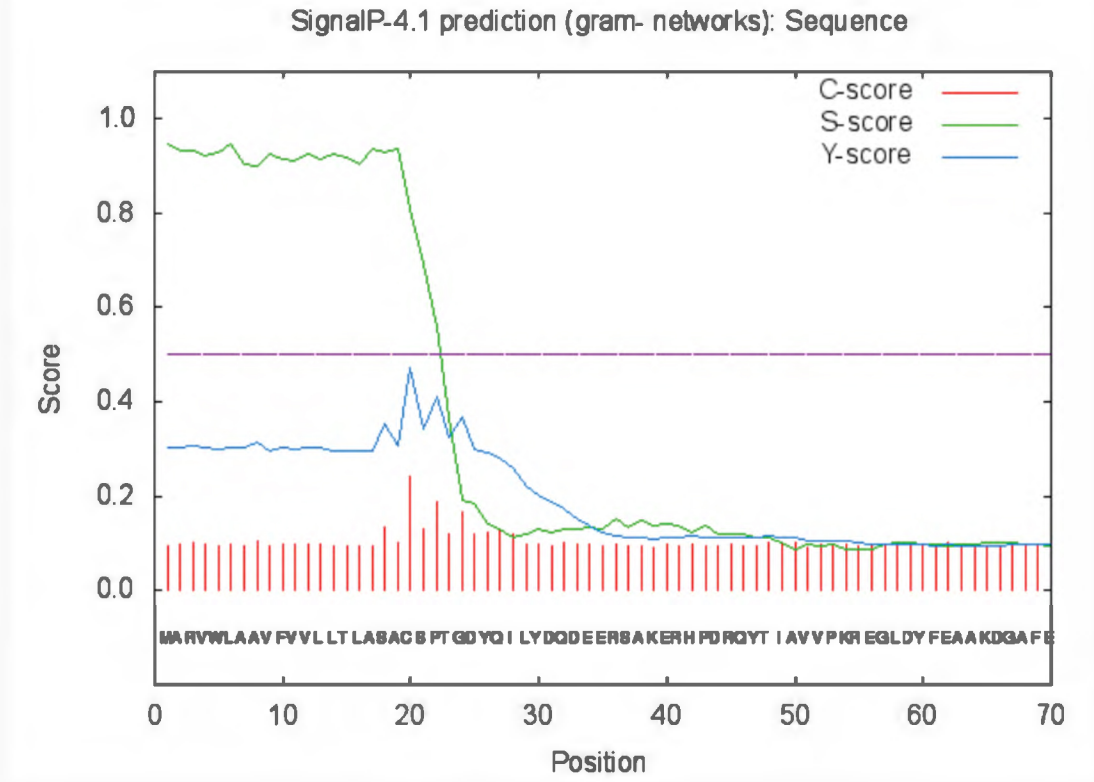


```
# Measure  Position  Value    Cutoff   signal peptide?
  max. C    20        0.242
  max. Y    20        0.472
  max. S     6        0.945
  mean S     1-19     0.923
       D     1-19     0.684   0.570    YES
Name=Sequence   SP='YES' Cleavage site between pos. 19 and 20: ASA-CS D=0.684 D-cutoff=0.570
```

Supplemental Figure 1 *SignalP prediction for signal sequence cleavage site for T. composti LsrB.*

Supplemental Figure 2 *Alignment of T. composti LsrB (cyan) with S. typhimurium LsrB (grey). The N-terminus of T. composti LsrB is residue 41, which corresponds to the first residue in Truncation 2. The locations of Truncations 3-5 highlighted in red after positions 43, 46, and 48, respectively.*

Thermobacillus composti

Sequence ID: lcl|Query_44565 Length: 344 Number of Matches: 1

Range 1: 4 to 344

Score	Expect	Method	Identities	Positives	Gaps	Frame
119 bits(298)	9e-35()	Compositional matrix adjust.	103/374(28%)	164/374(43%)	46/374(12%)	

Features:

```
Query  6    VALALIGAMIFTTLVGC---GSSNTTTDTSTNSSKKGN-----VTVTFIPKLTGNAFFES  57
            V LA +  ++ T    C   G      D     S K        T+  +PK  G  +FE+
Sbjct  4    VWLAAVFVVLLTLASACSPTGDYQILYDQDEERSAKERHPDRQYTIAVVPKREGLDYFEA  63

Query  58   ANKGAQKYSEQWGFKVDYEGDANASAASQVSVINKAVQQGTNAICLSSVDAAGVKDALKA  117
            A  GA + +++ G  V + G   A A +Q+ VI + ++Q  + + +SS D   +   LK
Sbjct  64   AKDGAFEAAKELGVNVLFRGPETADADAQIRVIEELIEQDIDLLAVSSNDPKKLLPVLKR  123

Query  118  AADAGVTVTTWDSDVDPSVRKVMVSQGTPEQLGQMLVQMGYDSLKERGKDPEKDAIKYCW  177
            A+D  + V TWDSD D   R   ++   PE LG+ L+     S  ERG        K+
Sbjct  124  ASDNNIAVITWDSDTDEEGRAFFINMVDPETLGRHLMDTLAWSTGERG--------KFAI  175

Query  178  HYSNATVTDQNSW----QVEGEKYIKSKYPNWQNVAPDNYYSNQDA-EQAISVGESILSA  232
               + +  + N W    +V+ ++Y    YPN + V      +N D+ E+A +    +L +
Sbjct  176  MTGSLSAANLNEWMHWIKVQQQEY----YPNMELV---EIAANNDSYEEAYASAVRLLES  228

Query  233  HSDIDLIICNDSTALPGQAQAAQNKGLTAKNVTITGFASPNSMKQYCNDGILTRWGLWDC  292
            H D+  II N S   P  A+A +  G   + V + G ++PN M+   +DG +    LW
Sbjct  229  HPDLAGIIGNSSVGPPSAAKAVKEAGKQGE-VKVVGLSTPNLMRDALHDGTVQVITLWSP  287

Query  293  GIQGAMGCYMAYYIASGNSVKVGDKIEIPTVGTVEVMPNSVLDPKADDSDTSSGVVLLPE  352
               G +   +  +  G     G  +    VG V V        K D       +V++ E
Sbjct  288  KRLGYLTVALGKNLLDGTLPYDGQFVN--KVGNVRV--------KGD-------MVIMGE  330

Query  353  RTIFTKDNMNNYDF  366
               FTKDN++ YDF
Sbjct  331  PLDFTKDNVDQYDF  344
```

Supplemental Figure 3 *BLAST sequence alignment of C. saccharobutylicium LsrB with T. composti LsrB.*

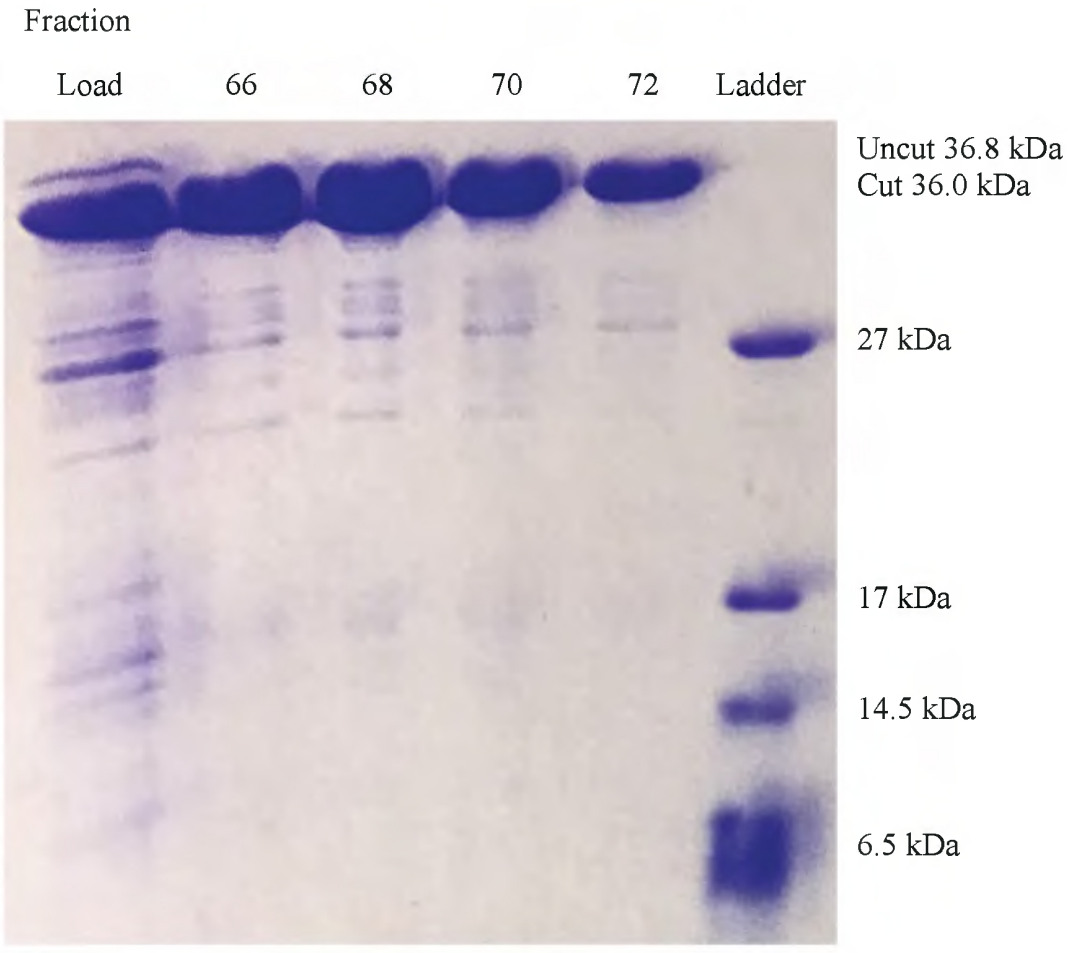

Supplemental Figure 4 *Gel of SourceQ purification of T. composti LsrB indicating that there was clean separation of cut and uncut protein.*

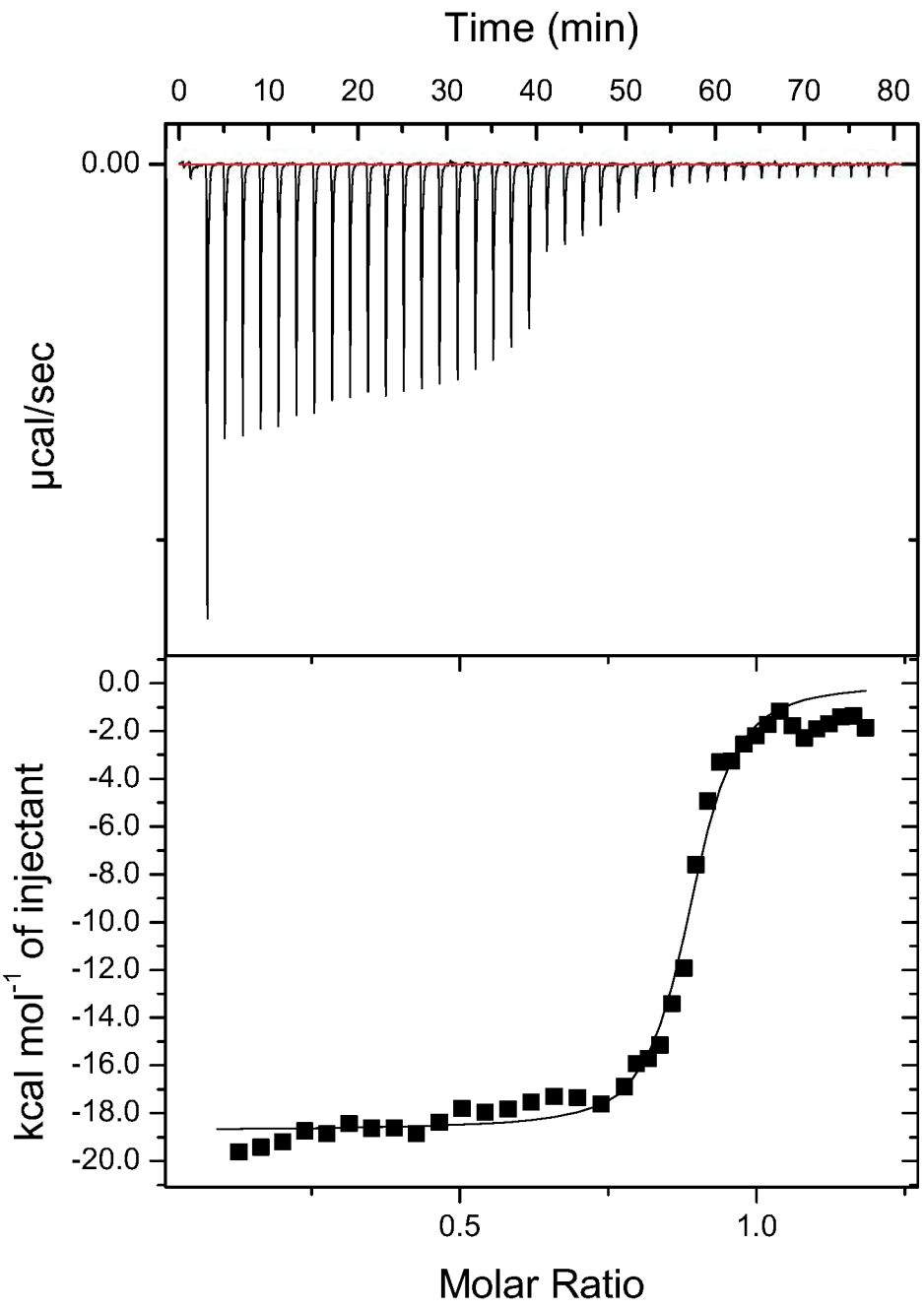

Supplemental Figure 5 *ITC titration of AI-2 into B. cereus LsrB. The K_D was determined to be 0.17±0.03 µM with an occupancy of 0.881±0.004.*

Supplemental Table 1 *Sorting of Index™ conditions with 40–60 mg·mL^{-1} T. composti LsrB.*

Condition	Salt			Buffer			pH	Precipitant		
I. CRASHED										
1				0.1	M	Citric acid	3.5	2.0	M	Ammonium sulfate
2				0.1	M	Sodium acetate trihydrate	4.5	2.0	M	Ammonium sulfate
7				0.1	M	Citric acid	3.5	3.0	M	Sodium chloride
8				0.1	M	Sodium acetate trihydrate	4.5	3.0	M	Sodium chloride
37								25	% w/v	Polyethylene glycol 1,500
40				0.1	M	Citric acid	3.5	25	% w/v	Polyethylene glycol 3,350
41				0.1	M	Sodium acetate trihydrate	4.5	25	% w/v	Polyethylene glycol 3,350
64	0.005	M	Cobalt(II) chloride hexahydrate	0.1	M	HEPES	7.5	12	% w/v	Polyethylene glycol 3,350
	0.005	M	Nickel(II) chloride hexahydrate							
	0.005	M	Cadmium chloride hydrate							
	0.005	M	Magnesium chloride hexahydrate							
93	0.05	M	Zinc acetate dihydrate					20	% w/v	Polyethylene glycol 3,350
II. LIGHT PRECIPITATE										
3				0.1	M	BIS-TRIS	5.5	2.0	M	Ammonium sulfate
26								1.1	M	Ammonium tartrate dibasic pH 7.0
43				0.1	M	BIS-TRIS	6.5	25	% w/v	Polyethylene glycol 3,350
46				0.1	M	BIS-TRIS	6.5	20	% w/v	Polyethylene glycol monomethyl ether 5,000
47				0.1	M	BIS-TRIS	6.5	28	% w/v	Polyethylene glycol monomethyl ether 2,000

75	0.2	M	Lithium sulfate monohydrate	0.1	M	BIS-TRIS	6.5	25	% w/v	Polyethylene glycol 3,350
90	0.2	M	Sodium formate					20	% w/v	Polyethylene glycol 3,350
III. MEDIUM PRECIPITATE										
4				0.1	M	BIS-TRIS	6.5	2.0	M	Ammonium sulfate
5				0.1	M	HEPES	7.5	2.0	M	Ammonium sulfate
6				0.1	M	Tris	8.5	2.0	M	Ammonium sulfate
17							5.6	1.26	M	Sodium phosphate monobasic monohydrate
								0.14	M	Potassium phosphate dibasic
19							8.2	0.056	M	Sodium phosphate monobasic monohydrate
								1.344	M	Potassium phosphate dibasic
51	0.2	M	Ammonium acetate	0.1	M	BIS-TRIS	6.5	45	% v/v	(+/-)-2-Methyl-2,4-pentanediol
58				0.1	M	BIS-TRIS	6.5	45	% v/v	Polypropylene glycol P 400
65	0.1	M	Ammonium acetate	0.1	M	BIS-TRIS	5.5	17	% w/v	Polyethylene glycol 10,000
66	0.2	M	Ammonium sulfate	0.1	M	BIS-TRIS	5.5	25	% w/v	Polyethylene glycol 3,350
76	0.2	M	Lithium sulfate monohydrate	0.1	M	HEPES	7.5	25	% w/v	Polyethylene glycol 3,350
82	0.2	M	Magnesium chloride hexahydrate	0.1	M	BIS-TRIS	5.5	25	% w/v	Polyethylene glycol 3,350
IV. HEAVY PRECIPITATE										
20				0.1	M	HEPES	7.5	1.4	M	Sodium citrate tribasic dihydrate
21								1.8	M	Ammonium citrate tribasic pH 7.0
23								2.1	M	DL-Malic acid pH 7.0

27								2.4	M	Sodium malonate pH 7.0
29								60	% v/v	Tacsimate pH 7.0
48	0.2	M	Calcium chloride dihydrate	0.1	M	BIS-TRIS	5.5	45	% v/v	(+/-)-2-Methyl-2,4-pentanediol
49	0.2	M	Calcium chloride dihydrate	0.1	M	BIS-TRIS	6.5	45	% v/v	(+/-)-2-Methyl-2,4-pentanediol
V. PHASE SEPARATION										
42				0.1	M	BIS-TRIS	5.5	25	% w/v	Polyethylene glycol 3,350
50	0.2	M	Ammonium acetate	0.1	M	BIS-TRIS	5.5	45	% v/v	(+/-)-2-Methyl-2,4-pentanediol
52	0.2	M	Ammonium acetate	0.1	M	HEPES	7.5	45	% v/v	(+/-)-2-Methyl-2,4-pentanediol
53	0.2	M	Ammonium acetate	0.1	M	Tris	8.5	45	% v/v	(+/-)-2-Methyl-2,4-pentanediol
54	0.05	M	Calcium chloride dihydrate	0.1	M	BIS-TRIS	6.5	30	% v/v	Polyethylene glycol monomethyl ether 550
55	0.05	M	Magnesium chloride hexahydrate	0.1	M	HEPES	7.5	30	% v/v	Polyethylene glycol monomethyl ether 550
59	0.02	M	Magnesium chloride hexahydrate	0.1	M	HEPES	7.5	22	% w/v	Polyacrylic acid sodium salt 5,100
70	0.2	M	Sodium chloride	0.1	M	BIS-TRIS	5.5	25	% w/v	Polyethylene glycol 3,350
71	0.2	M	Sodium chloride	0.1	M	BIS-TRIS	6.5	25	% w/v	Polyethylene glycol 3,350
72	0.2	M	Sodium chloride	0.1	M	HEPES	7.5	25	% w/v	Polyethylene glycol 3,350
74	0.2	M	Lithium sulfate monohydrate	0.1	M	BIS-TRIS	5.5	25	% w/v	Polyethylene glycol 3,350
78	0.2	M	Ammonium acetate	0.1	M	BIS-TRIS	5.5	25	% w/v	Polyethylene glycol 3,350
79	0.2	M	Ammonium acetate	0.1	M	BIS-TRIS	6.5	25	% w/v	Polyethylene glycol 3,350
83	0.2	M	Magnesium chloride hexahydrate	0.1	M	BIS-TRIS	6.5	25	% w/v	Polyethylene glycol 3,350
84	0.2	M	Magnesium chloride hexahydrate	0.1	M	HEPES	7.5	25	% w/v	Polyethylene glycol 3,350

85	0.2	M	Magnesium chloride hexahydrate	0.1	M	Tris	8.5	25	% w/v	Polyethylene glycol 3,350
91	0.15	M	DL-Malic acid pH 7.0					20	% w/v	Polyethylene glycol 3,350
92	0.1	M	Magnesium formate dihydrate					15	% w/v	Polyethylene glycol 3,350
95	0.1	M	Potassium thiocyanate					30	% w/v	Polyethylene glycol monomethyl ether 2,000
96	0.15	M	Potassium bromide					30	% w/v	Polyethylene glycol monomethyl ether 2,000

Supplemental Table 2 *Sorting of PEG R_x™ 1 conditions with 40–60 mg·mL^{-1} T. composti LsrB.*

PEG R_x 1

Condition	Buffer			pH	Polymer		
I. LIGHT PRECIPITATE							
33	0.1	M	Tris	8.0	28	% w/v	Polyethylene glycol 4,000
35	0.1	M	BIS-TRIS	6.5	20	% w/v	Polyethylene glycol monomethyl ether 5,000
37	0.1	M	Sodium citrate tribasic dihydrate	5.0	10	% w/v	Polyethylene glycol 6,000
38	0.1	M	Imidazole	7.0	20	% w/v	Polyethylene glycol 6,000
II. MEDIUM PRECIPITATE							
42	0.1	M	HEPES	7.5	4	% w/v	Polyethylene glycol 8,000
III. HEAVY PRECIPITATE							
4	0.1	M	Sodium acetate trihydrate	4.5	30	% v/v	Polyethylene glycol 300
13	0.1	M	Sodium acetate trihydrate	4.0	10	% v/v	Jeffamine® M-600® pH 7.0
19	0.1	M	Sodium acetate trihydrate	4.5	30	% w/v	Polyethylene glycol 1,500
43	0.1	M	Sodium acetate trihydrate	4.5	10	% w/v	Polyethylene glycol 10,000
IV. PHASE SEPARATION							
39	0.1	M	BIS-TRIS propane	9.0	30	% w/v	Polyethylene glycol 6,000
46	0.1	M	Sodium citrate tribasic dihydrate	5.0	18	% w/v	Polyethylene glycol 20,000

Supplemental Table 3 *Sorting of PEG R_x™ 2 conditions with 40–60 mg·mL^{-1} T. composti LsrB.*

PEG R_x 2

Condition	Buffer			pH	Polymer			Additive		
I. CRASHED										
4	0.1	M	BIS-TRIS	6.5	3	% v/v	Polyethylene glycol 200	28	% v/v	2-Propanol
47	0.1	M	Sodium citrate tribasic dihydrate	5.0	10	% w/v	Polyethylene glycol 20,000	0.2	M	Magnesium chloride hexahydrate
II. LIGHT PRECIPITATE										
6	0.1	M	Sodium citrate tribasic dihydrate	5.0	26	% v/v	Polyethylene glycol 400	10	% v/v	2-Propanol
29	0.1	M	MES monohydrate	6.0	25	% w/v	Polyethylene glycol 4,000	6	% v/v	Tacsimate pH 6.0
III. HEAVY PRECIPITATE										
3	0.1	M	MES monohydrate	6.0	45	% v/v	Polyethylene glycol 200	0.05	M	Calcium chloride dihydrate
IV. PHASE SEPARATION										
11	0.1	M	BIS-TRIS	6.5	2	% v/v	Polyethylene glycol monomethyl ether 550	1.8	M	Ammonium sulfate
21	0.1	M	MES monohydrate	6.0	20	% w/v	Polyethylene glycol monomethyl ether 2,000	20	% v/v	2-Propanol
23	0.1	M	BIS-TRIS propane	9.0	2	% w/v	Polyethylene glycol monomethyl ether 2,000	4.0	M	Potassium formate
28	0.1	M	Sodium citrate tribasic dihydrate	5.5	20	% w/v	Polyethylene glycol 4,000	18	% v/v	2-Propanol
31	0.1	M	Imidazole	7.0	24	% w/v	Polyethylene glycol monomethyl ether 5,000	2	% v/v	Polyethylene glycol 400
33	0.1	M	BIS-TRIS propane	9.0	20	% w/v	Polyethylene glycol monomethyl ether 5,000	4	% v/v	2-Propanol
39	0.1	M	BIS-TRIS propane	9.0	18	% w/v	Polyethylene glycol 8,000	10	% v/v	Polyethylene glycol 200
40	0.1	M	Sodium citrate tribasic dihydrate	5.0	10	% w/v	Polyethylene glycol 10,000	15	% v/v	2-Propanol
46	0.1	M	Sodium acetate trihydrate	4.5	2	% w/v	Polyethylene glycol 20,000	1.0	M	Sodium malonate pH 5.0